Detailed Analysis of the Relation Between Bipolar Electrode Spacing and Far- and Near-Field Electrograms

Masateru Takigawa, Jatin Relan, Ruairidh Martin, Steven Kim, Takeshi Kitamura, Ghassen Cheniti, Konstantinos Vlachos, Xavier Pillois, Antonio Frontera, Grégoire Massoullié, et al.

Detailed Analysis of The Relation between Bipolar Electrode Spacing and Far- and Near-Field Electrograms

Masateru Takigawa,MD,PhD[*1,2]; Jatin Relan,MD,PhD[*1,3]; Ruairidh Martin,MD[*1,4]; Steven Kim,MD,PhD[3]; Takeshi Kitamura,MD[1]; Ghassen Cheniti,MD[1]; Konstantinos Vlachos,MD,PhD[1]; Xavier Pillois,PhD[1]; Antonio Frontera,MD[1]; Grégoire Massoullié,MD[1]; Nathaniel Thompson,MD[1]; Claire A Martin,MD,PhD[1], Felix Bourier,MD,PhD[1]; Anna Lam,MD[1]; Michael Wolf,MD[1]; Josselin Duchateau,MD[1]; Nicolas Klotz,MD[1]; Thomas Pambrun,MD[1]; Arnaud Denis,MD[1]; Nicolas Derval,MD[1]; Julie Magat,PhD[1], Jérôme Naulin,MSc[1], Mathilde Merle,MSc[1], Florent Collot,MSc[1], Bruno Quesson,PhD[1]; Hubert Cochet,MD, PhD[1]; Mélèze Hocini,MD[1], Michel Haïssaguerre,MD[1]; Frederic Sacher,MD,PhD[1]; Pierre Jaïs,MD[1].

Running Title: Impact of Bipolar Spacing on EGMs

[1]CHU Bordeaux, IHU Lyric, Université de Bordeaux, Bordeaux, France
[2]Heart Rhythm Center, Tokyo Medical and Dental university
[3]Abbott, MN, USA
[4]Institute of Genetic Medicine, Newcastle University, Newcastle-upon-Tyne
[*]These authors contributed equally to this work.

FUNDING

Equipex MUSIC ANR-11-EQPX-0030, IHU LIRYC ANR-10-IAHU-04, research grant from Abbott.

DISCLOSURE

Drs Haïssaguerre, Hocini, Jaïs and Sacher:Lecture fees from Biosense Webster and Abbott. Drs Denis, Derval, Jaïs and Sacher:Speaking honoraria/consulting fees from Boston Scientific.

Mrs Jatin and Kim:Employees of Abbott.

Correspondence

Masateru Takigawa

CHU Bordeaux, IHU Lyric, Université de Bordeaux

Avenue de Magellan, 33604 Bordeaux-Pessac, France.

Phone/Fax: +330556795679

Email: teru.takigawa@gmail.com

ABSTRACT
Background: Detailed effect of bipolar spacing on electrograms (EGMs) is not well described.
Method: With a HD-Grid catheter, EGMs from different bipole pairs can be created in each acquisition. We analyzed the effect of bipolar spacing on elecrograms in 7 infarcted sheep. A segment was defined as a 2mm center-to-center bipole. In total, 4768 segments (2020 healthy, 1542 scar, and 1206 in border areas, defined by MRI) were covered with an electrode pair of spacing 2mm (Bi-2), 4mm (Bi-4), and 8mm (Bi-8).
Results: 3591 segments in Bi-2 were free from local abnormal ventricular activities (LAVAs); 1630 segments were within the MRI-defined scar/border area. Among them, 172 (10.6%) segments in Bi-4, and 219 (13.4%) segments in Bi-8 showed LAVAs. In contrast, LAVAs were identified in 1177 segments in Bi-2; 1118 segments were within the MRI-defined scar/border area. Among them, LAVAs were missed in 161 (14.4%) segments in Bi-4, and 409 (36.6%) segments in Bi-8.
In segments with LAVAs, median far-field voltage increased from 0.09[0.06-0.14]mV in Bi-2, to 0.16[0.10-0.24]mV in Bi-4, and 0.28[0.20-0.42]mV in Bi-8 (P<0.0001). Median near-field voltage increased from 0.14[0.08-0.25]mV in Bi-2, to 0.21[0.12-0.35]mV in Bi-4, and 0.32[0.17-0.48]mV in Bi-8 (P<0.0001). Median near/far-field voltage ratio decreased from 1.67 in Bi-2, to 1.43 in Bi-4, and 1.23 in Bi-8 (P<0.0001).
Conclusion: Closer spacing better discriminates dead scar from surviving tissue. While far-field voltage systematically increases with spacing, near-field voltages were more variable, depending on local surviving muscular bundles. Near-field EGMs are more easily observed with smaller spacing, largely due to the reduction of far-field effect.
Keywords; electrograms; high-density mapping; multipolar catheters; LAVA
CONDENSED ABSTRACT
We compared EGMs on each given site in the same beat with different spacing bipolar pairs, using HD-grid catheter, demonstrating the following findings.
(1) Increased spacing may miss LAVA areas and also mistakenly identifying scar or normal tissue areas as having LAVAs
(2) Generally, both far- and near- field voltage may increase as the spacing increases. However, near-field increase may be less proportional
(3) Near-field/far-field voltage ratio increases as the spacing decreases due to the predominant reduction of far-field effect.
(4) In pure scar areas, local voltages were additively increased as the spacing increases, however local voltages in the healthy tissue were more heterogenous.
Abbreviations and acronyms

CS: coronary sinus

EAM: electro anatomical mapping

EGM: electrocardiogram

LV: left ventricle

LAVA: local abnormal ventricular activities

MRI: magnetic resonance imaging

VT: ventricular tachycardia

INTRODUCTION

Bipolar mapping of ventricular scar has previously been validated with focal ablation catheters as well as multi-polar catheters.(1-3) Multipolar mapping are increasingly being used for substrate delineation. They offer faster and higher density map(4-6) expected to be superior to those obtained using ablation catheters. However, the impact of interelectrode spacing on bipole electrograms (EGMs) in the ventricle has not been systematically examined. This seems particularly important as ablation targets are determined by the signal recoded during the mapping phase, whether it consist in activation or voltage map. The aims of the present study were to delineate the effect of increasing inter-electrode spacing on local (far- and near- field) EGMs, with reference to scar regions defined by magnetic resonance imaging (MRI).

METHODS

Experimental myocardial infarction

Experimental protocols were conducted in compliance with the Guiding Principles in the Use and Care of Animals published by the National Institutes of Health (NIH Publication No. 85-23, Revised 1996). Additionally, the study was approved by the institutional animal use and care committee in addition to conforming to the guide for the care and use of laboratory animals. Seven female sheep (age 4.1years, 54.9±6.9kg) were sedated with an intramuscular injection of ketamine hydrochloride (20mg/kg), acepromazine (0.1mg/kg), and buprenorphine (20ug/kg). After the intravenous injection of propofol (2mg/kg), sheep was intubated and anesthesia was maintained with 2-3% isoflurane. Sheep were ventilated with the respirator (CARESTATION/Carescape GE, Chicago, US), using room air supplemented with oxygen. An intravenous catheter was placed in the internal jugular vein for infusion of drugs and fluids. Arterial blood gases were monitored periodically, and ventilator parameters were adjusted to maintain blood gases within physiological ranges. A sheep myocardial infarction model was created by an experienced invasive cardiologist using selective ethanol

injection (1–2 cc) in the distal 1/3rd of the left anterior descending artery.

MRI myocardial scar segmentation

Late gadolinium-enhanced cardiac MRI was performed 2-3 months after the creation of myocardial infarction. Image processing was performed by 2 trained technicians using the MUSIC software (EQUIPEX MUSIC, Liryc, Universite´ de Bordeaux/INRIA, Sophia Antipolis, France). Segmentation was performed as described previously.(7,8) Briefly, the cardiac chambers, ventricular epicardium, ascending aorta, and coronary sinus (CS) were segmented using semi-automatic methods.(8) From left ventricular (LV) wall segmentation, adaptive histogram thresholding was applied in order to segment dense scar (threshold set at 50% maximum signal intensity) and grey zone (from 35 to 50%)(9-11).

Electrophysiological study and mapping with HD-Grid™ Catheter

Electrophysiological study with HD-Grid™ catheter (Abbott, Minneapolis, MN, USA, Figure 1A) was performed 1-3 days after the MRI examination in surviving post-infarct sheep with an identical sedation, analgesia, intubation, and ventilation protocol for mapping of the scar using a three dimensional electroanatomical mapping (3D-EAM) (NavX Precision system, research version, Abbott, MN, USA) (Figure 1A). A diagnostic catheter (quadripolar catheter, Boston Scientific) was placed in right ventricle and CS. The LV was mapped with HD-Grid™ catheter (3-mm interelectrode spacing and 1-mm electrode size) via a retrograde aortic approach and/or transseptal approach. A steerable long sheath (Agilis, Abbott, Minneapolis, MN, USA) was used if required. The internal projection setting was set at 7 mm with 10-mm interpolation. Field-scaling was applied for all maps. On the point acquisition, contact to the LV endocardial surface was confirmed by fluoroscopy and the proximity indicator on the NavX-Precision™ system (Agilis, Abbott, Minneapolis, MN, USA). In addition, the research version of this system included two features to convince the contact; one feature was to show the catheter placement in each beat, and the other was to allow the system to display whether electrodes of the multipolar catheter were in contact with the tissue based on the

impedance information (Supplemental figure). The beat was not acquired when the catheter was distorted, being trapped in particular space such as the papillary muscles, valves, trabeculations or when adjacent two splines touched each other, causing noises.

For the registration, all segmentations of MRI imaging were exported as meshes and loaded into the NavX system. The registration algorithm with the Ensite-NavX™ Fusion™ module allowed dynamic molding of the 3D-EAM geometry onto the MRI surface.(12) After primary registration, the registered model was refined using a second set of fiducial points such as left atrium, CS, aortic root, LV apex, and mitral annulus, judiciously placed in a stepwise fashion to further align both surfaces at sites of local mismatch (Figure 1B).

EGM analysis

With a HD-Grid™ catheter, different bipolar pairs can be selected. To assess the effect of bipolar spacing, specific configuration was created using electrodes 1 to 5 in each spline (Figure 1A). The 2-mm bipole pair (Bi-2, 2mm center to center, 1mm edge-to-edge) was created from electrodes 1-2, 2-3, 3-4, and 4-5 in each spline, which was defined as the smallest segment. Bi-2 was compared to the 4-mm bipole pair (Bi-4, 4mm center to center, 3mm edge-to-edge) created from electrodes1-3 and 3-5 in each spline. We also used the 8-mm bipole pair (Bi-8, 8mm center-to-center, 7mm edge-to-edge) created from electrodes 1-5. (Figure 1A). In each beat acquisition, EGMs created by 2, 4, and 8mm center-to-center spacing covering exactly the same site was compared; Four Bi-2 segments are compared with two Bi-4 and one Bi-8 recordings. Bipolar EGMs were filtered at 30-300Hz. HD-32 (4 splines) was used in sheep 1-5, and HD-56 (7 splines) was prepared for the study. Importantly, HD-32 and HD-56 have the same electrode spacing (and electrode size only

differing by the number of splines. Again, each portion between adjacent electrodes on the spline was defined as 1 segment and the region covered between electrode 1 and 5 was defined as 1 site (Figure 1B). We arbitrarily defined Bi-2 as the reference, and compared the following between three different bipolar spacing in each MRI-defined region.

1. Detection of local abnormal ventricular activities (LAVAs)
2. Changes in EGMs at sites where far- and near-field potentials were separately measured.
3. Changes in single potentials in purely healthy and purely scar areas.

Our definition of LAVA has been described previously.(5) LAVAs are defined as sharp high-frequency ventricular potentials, possibly of low amplitude (but not always), distinct from the far-field ventricular EGMs. They sometimes display fractionation, double, or multiple components separated by very-low-amplitude EGMs or an isoelectric interval, and are poorly coupled to the rest of the myocardium. In case the discrimination of far- and near-field EGMs were difficult, programmed ventricular stimulation or local pacing with decremental output was performed. LAVA analysis was performed manually by two independent, blinded physicians.

Statistical analysis

Data are expressed as mean±standard deviation and/or [median;25th-75th percentile] for normally distributed and skewed data, respectively. For the comparison of three groups, Steel-Dwass analysis was performed. P-values<0.05 were considered statistically significant.

RESULTS

EGM acquisition

EGMs were collected during sinus rhythm (SR) in 5 sheep and right ventricular pacing in the remaining 2 because of frequent mechanical ventricular rhythm during sinus rhythm (Table1). In total, 4768 segments were analyzed by Bi-2, Bi-4, and Bi-8. 2020 segments were in MRI defined

healthy area, 1542 segments were in MRI-defined scar area, and 1206 segments were in MRI-defined grey areas (border area).

Overlooking true scars with increased bipole spacing (Figure 2A)

3591 segments were LAVA free with Bi-2. Yet, in 181 (5.0%) segments analyzed with Bi-4, and 228 (6.3%) with Bi-8, LAVAs were recorded as a consequence of the larger antenna of the bipoles. In MRI-defined scar area, single component EGMs without LAVAs were identified in 818 segments with Bi-2. However, in 113 (13.8%) segments analyzed with Bi-4, and 116 (14.2%) segments with Bi-8 LAVAs were recorded for the same reason (Figure 2B). In MRI-defined border area, 812 segments were LAVA-free in Bi-2, of which 59 (7.3%) segments in Bi-4, and 103 (12.7%) segments in Bi-8 showed LAVAs. In MRI-defined healthy area, 1961 segments were LAVA-free with Bi-2, of which 9 (0.5%) segments with Bi-4, and 9 (0.5%) segments with Bi-8 showed multiple components.

Overlooking LAVAs with increased bipole spacing (Figure 3A)

LAVAs were identified in 1177 segments in Bi-2. Two hundred and two (17.2%) of these segments in Bi-4, and 449 (38.1%) in Bi-8 missed these LAVAs. In MRI-defined scar areas, LAVAs were identified in 724 segments with Bi-2. Seventy-nine (10.9%) of these segments in Bi-4, and 236 (32.6%) in Bi-8 missed these LAVAs. In MRI-defined border areas, LAVAs were identified in 394 segments in Bi-2. One hundred (25.4%) of these segments in Bi-4, and 173 (43.9%) in Bi-8 missed these LAVAs (Figure 3B). In MRI-defined healthy area, multiple component EGMs were identified in 59 segments in Bi-2 mostly around the mitral valve, while 23 (39.0%) of these segments in Bi-4, and 40 (67.8%) in Bi-8 showed single component potentials.

Near-field/far-field voltage ratio decreases with spacing

In total, 1177 segments in Bi-2, 1156 segments in Bi-4, and 956 segments in Bi-8 showed both far-field and near-field EGMs. In general, mean far-field voltage significantly increased as the spacing increased as shown in Figure 4A-(a) ($P<0.0001$). The tendency was similar in MRI-defined healthy area, MRI-defined border area, and MRI-defined scar area (Figure 4B-(a), 4C-(a), and

4D-(a)). In general, mean near-field voltage became significantly larger as the spacing increased as shown in Figure 4A-(b) ($P<0.0001$), but the extent of the increase was smaller than the far-field, and the far-field showed more proportional increase with the spacing; The increase did not reach significance in Bi-2 vs. Bi-4, and Bi-4 vs. Bi-8, in MRI-defined border area. (Figure 4C-(a)).

In general, mean near-field/far-field voltage ratio significantly decreased as the spacing increased as shown in Figure 4A-(c) ($P<0.0001$). The tendency was similar in MRI-defined border and scar areas (Figure 4C-(c), and 4D-(d)).

Relation between spacing and voltage in purely healthy and purely scarred areas.

We defined as purely healthy 1856 segments where electrodes 1 to 5 in one spline were all simultaneously in an MRI-defined healthy area, without LAVAs. We defined as purely scarred 228 segments where electrodes 1 to 5 in one spline were all simultaneously in an MRI-defined scar area without LAVAs.

In the purely scarred area, median voltage significantly ($P<0.0001$) increased from 0.13mV to 0.26mV in Bi-4, and 0.51mV in Bi-8 as shown in Figure 5A. Adding the voltage of two or four adjacent 2-mm bipoles (Bi-2) included in the corresponding Bi-4 or Bi-8 resulted in almost the same voltage ($R^2=0.99$, $R^2=0.98$, respectively) (Figure 5B, C).

In the purely healthy area, median signal voltage increased from 1.18mV in Bi-2, to 1.81mV in Bi-4, and 2.58mV in Bi-8 as shown in Figure 6A. Adding the voltage of two or four adjacent 2-mm bipoles (Bi-2) included in the corresponding Bi-4 or Bi-8 was more weakly correlated to the voltage in Bi-4 ($R^2=0.82$) and Bi-8 ($R^2=0.64$), (Figure 6B, C).

DISCUSSION

Major findings

In the present study, we examined EGMs in the same beat with the different spacing bipolar pairs and demonstrated the following findings.

1.Widely spaced bipoles may fail to discriminate the local tissue characteristics; increased spacing may result in missing LAVA areas and mistakenly identifying scar or normal tissue areas as having LAVAs.

2.Although, generally, both far- and near- field voltage may increase as the spacing increases, near-field increase may be less proportional.

3.Near-field/far-field voltage ratio increases as the spacing decreases due to the predominant reduction of far-field effect.

4.In pure scar areas, local voltages were additively increased as the spacing increases, however local voltages in the healthy tissue were more heterogenous.

LAVA detection accuracy with bipolar spacing

In the present study, we have demonstrated that LAVA potentials detected by the closest spacing (Bi-2) might be missed in Bi-4 by 17.2%, and in Bi-8 by 38.1%. And this false-negative rate is generally higher in the MRI-defined border area than the dense scar area. LAVA timing is reported to be earlier in the border zone than in dense scar area(13), and early LAVA in sinus rhythm may be associated with channels entering into the scar(14). In these border zones, far-field EGMs are larger due to adjacent healthy tissue. With widely-spaced bipoles, some LAVAs detected with Bi-2 may be masked and therefore missed by large far-field EGMs (as shown in Figure 3E).

On the other hand, where single potentials were detected with the smallest bipolar spacing (Bi-2), 5% with Bi-4 and 6% with Bi-8 had LAVAs with far- and near-field EGMs. Particularly in MRI-defined scar areas, where the incidence of LAVAs increases to 13.8% by Bi-4 and 14.2% by Bi-8. This does not suggest that larger spacing bipoles detect LAVAs better, but rather that widely-spaced bipoles indiscriminately detect LAVA EGMs across the entire bipole, which smaller bipole pairs are able to pinpoint more accurately, as shown in Figure 2E. And even if larger bipoles are not as accurate as smaller ones, they may still be useful, for example in identifying an interesting

electrogram that is nearby but not right under the spline.

Voltage changes in far- and near- field potentials.

Two previous studies have demonstrated that bipolar voltages, in general, increase with spacing[13,14]. Neither study compared identical sites simultaneously, however, nor did they discriminate between near-field and far-field EGMs(15,16). Furthermore, the comparison between different catheters may have affected the result because of the different electrode size and shape(16). In the present study, by comparing EGMs with a different spacing at exactly the same location (site) and beat, the exact effect of bipolar spacing was clearly described. We have demonstrated that both far- and near-field voltages generally increases with spacing, and that this rule is generally consistent in MRI-defined scar and border areas. However, the voltage increases greater in far-field EGMs with longer spacing, thus the near-field/far-field voltage ratio being decreased, resulting in worse discrimination between near-field and far-field EGMs.

Correlation between bipolar spacing and voltage

In purely scarred areas, the additive voltage of Bi-2 was equal to the voltage of Bi-4, and Bi-8 with a good correlation. The (electrode center to center) spacing may be additively associated with far-field voltages, and the correlation coefficient is very high. In contrast, in purely healthy areas, although there is a correlation between the additive voltage of smallest bipolar spacing (Bi-2) and the other spacing, the correlation coefficient was not as directly proportional as in the purely scarred area. This discrepancy may be because of the fact that single components in the purely scarred area may represent the pure far-field EGMs, whereas single component EGMs in the purely healthy areas may represent both far-field and near-field components, which will not simply be summed over a longer bipole.

In segments where both far- and near- field EGMs were identified, far-field EGMs tended to increase with spacing. However, the extent was not as directly proportional as in completely scarred areas. This may be due to the presence of some near-field component in the far-field signal. Another hypothesis is that in the border zone, far-field effect can be produced both from the horizontal direction and the vertical direction (Sub-endocardial surviving tissues), while in the complete scar zone, far-field effect from the vertical direction may be less.

The change in the near-field voltages according to bipolar spacing was less proportional compared to the far-field EGMs, especially in the border zone. In some cases, the voltages are similar even when the spacing was increased (as shown in Figure 2E). If there is only a single piece of surviving muscle, covered by one segment with Bi-2, this signal voltage may not change dramatically in Bi-4 or Bi-8 when the other segments are all scar. When the surviving muscular bundle is large enough to extend beyond a single 2mm segment however, the near-field signal will increase with a longer bipolar spacing. In addition, near-field voltage is more sensitive to the relation between, bipolar orientation, tissue orientation, and activation direction, which could more affect the near-field EGMs.(17)

Clinical Implications

Mapping during ventricular tachycardia (VT) can be performed in only 30% to 40% of cases.(18) Therefore detection and characterization of myocardial scar during sinus rhythm may be a prerequisite for substrate-based scar modification in some patients. For this substrate-based scar modification, several techniques have been reported, such as scar de-channeling(19), late potential ablation(20), scar homogenizing(21), and LAVA elimination(5). In all of these techniques, residual abnormal muscle bundles in the scar which are potentially associated with the initiation or maintenance of VT are targeted. These tissues usually have small sharp EGMs, which are occasionally masked by the far-field component.(5) Detection and discrimination of these near-field EGMs from the far-field EGMs is mandatory for these techniques. We have demonstrated that catheters with smaller bipolar spacing may achieve the precise discrimination of the local tissue

structures. In addition, we elucidated the impact of bipolar spacing on both far- and near-field EGMs. Recently, industry has provided new technologies including several types of multipolar mapping catheters with different electrode size and different inter-electrode spacing (eg. PentaRay® [electrode size: 3.14mm^2, (center-to-center) inter-electrode spacing: 3mm], Biosense-Webster Inc., Diamond Bar, CA; and OrionTM [electrode size:0.4mm^2, (center-to-center) inter-electrode spacing: 2.5mm], Boston Scientific, Marlborough, MA). Although larger electrode and larger inter-electrode spacing may increase the far-field effect, the impact on the EGMs in these different technologies should be examined. In addition, a specific scar threshold should be determined in each different catheter platform, although, 0.5mV< and 1.5mV> have been, so far, generally used for the threshold of dense scar and healthy voltages, respectively.

Limitations

First, LAVA analysis was performed manually. In order to minimize bias when identifying LAVAs, analysis was performed by two independent, blinded physicians with adjudication by a third physician where there was disagreement. Second, contact force is known to impact recorded EGMs but no multipolar mapping catheters are capable of contact force measurement. Intracardiac echocardiography might have been a better method to minimize this limitation. Third, although the histology and pathology was not compared to the MRI-defined scar in the present study, the well-known cut-off of MRI-defined scar was used for the analysis (9-11). Fourth, as EGMs during sinus rhythm and RV pacing were mixed for the analysis, local voltages may be affected. Finally, this study did not include epicardial mapping, which may have resulted in different EGM characteristics, due to the impact of epicardial fat.

CONCLUSION

Closer spacing is superior for identifying surviving tissue in the scar. Far-field voltage increases additively with spacing while near-field voltages are more sensitive to the tissue heterogeneity.

Near-field EGMs are more easily identified with smaller spacing, particularly due to the reduction of far-field effect in scar.

PERSPECTIVES

COMPETENCY IN MEDICAL KNOWLEDGE:

High-resolution mapping with smaller spacing provides a more accurate characterization in the infarcted scar associated with the VT substrate. Better understanding of the substrate will provide the appropriate ablation strategy without unnecessary RF applications. Understanding of the effect of inter-electrode spacing on both far- and near-field electrograms must be required in the era when the advancing technology in the industry may provide different types of catheters.

TRANSLATIONAL OUTLOOK-1: Although the high-resolution mapping catheter will for sure provide more precise characteristics of substrates of ventricular tachycardia, the clinical impact should be examined in further studies.

TRANSLATIONAL OUTLOOK-2: Lack of contact force in mapping catheters may limit the advantage of high-resolution mapping system. A larger bipole but with contact-force vs a smaller bipole without contact-force should be examined.

REFERENCES

1. Callans DJ, Ren JF, Michele J, Marchlinski FE, Dillon SM. Electroanatomic left ventricular mapping in the porcine model of healed anterior myocardial infarction. Correlation with intracardiac echocardiography and pathological analysis. Circulation.1999;100:1744–1750.

2. Reddy VY, Wrobleski D, Houghtaling C, Josephson ME, Ruskin JN. Combined epicardial and endocardial electroanatomic mapping in a porcine model of healed myocardial infarction. Circulation.2003;107:3236–3242.

3. Tung R, Nakahara S, Ramirez R, et al. Accuracy of combined endocardial and epicardial electroanatomic mapping of a reperfused porcine infarct model: a comparison of electrofield and magnetic systems with histopathologic correlation. Heart Rhythm.2011;8:439–447.

4. Patel AM, d'Avila A, Neuzil P, et al. A trial tachycardia after ablation of persistent atrial fibrillation: identification of the critical isthmus with a combination of multielectrode activation mapping and targeted entrainment mapping. Circ Arrhythm Electrophysiol.2008;1:14–22.

5. Jaïs P, Maury P, Khairy P, et al. Elimination of local abnormal ventricular activities: a new endpoint for substrate modification in patients with scar-related ventricular tachycardia. Circulation.2012;125:2184–2196.

6. Tung R, Nakahara S, Maccabelli G, et al. Ultra high-density multipolar mapping with double ventricular access: a novel technique for ablation of ventricular tachycardia. J CardiovascElectrophysiol.2011;22:49–56.

7. Komatsu Y, Cochet H, Jadidi A, et al. Regional myocardial wall thinning at multidetector computed tomography correlates to arrhythmogenic substrate in postinfarction ventricular tachycardia: Assessment of structural and electrical substrate. Circ Arrhythm Electrophysiol.2013;6:342-350. □

8. Cochet H, Komatsu Y, Sacher F, et al. Integration of merged delayed-enhanced magnetic resonance imaging and multidetector computed tomography for the guidance of ventricular

tachycardia ablation: A pilot study. J Cardiovasc Electrophysiol.2013;24:419-426.

9. Amado LC, Gerber BL, Gupta SN, et al. Accurate and objective infarct sizing by contrast-enhanced magnetic resonance imaging in a canine myocardial infarction model. J Am Coll Cardiol.2004;44:2383-2389.

10. Olimulder MA, Kraaier K, Galjee MA, et al. Infarct tissue characterization in implantable cardioverter-defibrillator recipients for primary versus secondary prevention following myocardial infarction: a study with contrast-enhancement cardiovascular magnetic resonance imaging. Int J Cardiovasc Imaging.2013;29:169-176

11. Roes SD, Borleffs CJ, van der Geest RJ, et al. Infarct Tissue Heterogeneity Assessed With Contrast-Enhanced MRI Predicts Spontaneous Ventricular Arrhythmia in Patients With Ischemic Cardiomyopathy and Implantable Cardioverter-Defibrillator. Circ Cardiovasc Imaging.2009;2:183-190

12. West JJ, Patel AR, Kramer CM, et al. Dynamic registration of preablation imaging with a catheter geometry to guide ablation in a sheep model: validation of image integration and assessment of catheter navigation accuracy. *J Cardiovasc Electrophysiol*.2010;21:81–87.

13. Komatsu Y, Daly M, Sacher F, et al. Electrophysiologic characterization of local abnormal ventricular activities in postinfarction ventricular tachycardia with respect to their anatomic location. Heart Rhythm.2013;10:1630-1637.

14. Tung R, Mathuria NS, Nagel R, et al. Impact of local ablation on interconnected channels within ventricular scar: mechanistic implications for substrate modification. Circ Arrhythm Electrophysiol.2013;6:1131-1138.

15. Tung R, Kim S, Yagishita D, Vaseghi M, et al. Scar voltage threshold determination using ex vivo magnetic resonance imaging integration in a porcine infarct model: Influence of interelectrode distances and three-dimensional spatial effects of scar. Heart Rhythm.2016;13:1993-2002.

16. Berte B, Relan J, Sacher F, et al. Impact of electrode type on mapping of scar-related VT. J Cardiovasc Electrophysiol. 2015. doi: 10.1111/jce.12761.

17. Anter E, Josephson ME. Bipolar voltage amplitude: What does it really mean? Heart Rhythm. 2016;13:326-327.

18. Tung R, Vaseghi M, Frankel DS, et al. Freedom from recurrent ventricular tachycardia after catheter ablation is associated with improved survival in patients with structural heart disease: An International VT Ablation Center Collaborative Group study. Heart Rhythm.2015;12:1997–2007.

19. Berruezo A, Fernandez-Armenta J, Andreu D, et al. Scar dechanneling: new method for scar-related left ventricular tachycardia substrate ablation.Circ Arrhythm Electrophysiol.2015;8:326–36.

20. Silberbauer J, Oloriz T, Maccabelli G, et al. Noninducibility and late potential abolition: a novel combined prognostic procedural endpoint for catheter ablation of postinfarction ventricular tachycardia. Circ Arrhythm Electrophysiol.2014;7:424-435.

21. Di Biase L, Burkhardt JD, Lakkireddy D, et al. Ablation of Stable VTs Versus Substrate Ablation in Ischemic Cardiomyopathy: The VISTA Randomized Multicenter Trial. J Am Coll Cardiol.2015;66:2872-2882.

TABLES

Table 1A. Baseline Characteristics (N=7)

Sheep No	Sex	Age, yrs	Weight, kg	Rhythm	HD grid	Analyzed site	Analyzed segments
1	f	5	60	Sinus	HD-32	156	624
2	f	5	56.5	Sinus	HD-32	140	560
3	f	5	60	Sinus	HD-32	192	768
4	f	5	48	Sinus	HD-32	136	544
5	f	5	63	Sinus	HD-32	116	464
6	f	2	52	RV pacing	HD-56	154	616
7	f	2	44.6	RV pacing	HD-56	298	1192

Figure legends

Figure 1:Bipolar configuration on the HD-Grid™ catheter MRI-image registration.
The HD-Grid™ catheter has eight 1-mm electrodes with 1-mm spacing (edge-to-edge) in each spline. HD-32 mounts 4-splines, and HD-56 mounts 7-splines. 2-mm bipole pair (center to center) (Bi-2), which covers one segment, is created from electrodes 1-2, 2-3, 3-4, and 4-5 in each spline. The 4-mm bipole pair (Bi-4) is created from electrodes1-3 and 3-5 in each spline. The 8-mm bipole pair (Bi-8), which covers one site, is created from electrodes 1-5 (A). MRI-image with MRI-defined scar and grey area (border area) is merged in the 3D mapping system (B).

Figure 2:Overlooking true scars with increased bipolar spacing
The incidence of LAVAs in Bi-4 and Bi-8 in segments where Bi-2 does not show LAVAs in total (A), in MRI-defined healthy area (B), in MRI-defined border area (C), and in MRI-defined scar area (D). Figure (E) demonstrates that G2-3, G3-4, G4-5 shows scar tissue without LAVA but these dense scar spot was overlooked with larger spacing bipoles in Bi-4 (G1-3) and Bi-8 (G1-5). Note that the most closely spaced bipoles (Bi-2) clearly discriminated 3 scar segments and 1 living tissue segment at this catheter location. In contrast, larger bipolar catheters may inaccurately identify LAVAs at these locations. In addition, one can see large differences in far-field voltages between Bi-2 (G1-2), and Bi-4 (G1-3) and Bi-8 (G1-5), whereas near-field voltages do not change dramatically. Unipolar-G1, interestingly, displays the small local electrogram, possibly associated with LAVAs in bipoles. P;pacing artifact

Figure 3:Overlooking LAVAs with increased bipolar spacing.
The incidence of no LAVAs (dead area or heathy area) in Bi-4 and Bi-8 in segments where Bi-2 shows LAVAs in total (A), in MRI-defined healthy area (B), in MRI-defined border area (C), and in MRI-defined scar area (D). Figure (E) shows that D1-2, 2-3, 3-4, and 4-5 (Bi-2) have LAVAs which are not identified in D1-5 (Bi-8). Unipolar does not display EGMs associated with LAVAs shown in bipoles. P;pacing artifact

Figure 4:The effect of bipolar spacing on EGMs according to the MRI-defined area.
The effect of different bipolar spacing on far-field voltage (a) near-field voltage (b) and near-field/far-field voltage ratio (c) according to the MRI-defined area: Total (A), MRI-defined healthy area (B), MRI-defined border area (C), and MRI-defined scar area (D).

Figure 5:The relationship between voltage and spacing in purely scarred areas. Voltage comparison in scar areas with single component (Far-field only) without LAVAs between three different spacing (A). The relationship between additive bipolar voltage of Bi-2 and the bipolar voltage of Bi-4 (B) and Bi-8(C). An example of the voltages in one acquisition where all of electrodes 1-5 on one spline (spline G) were located in a scar area (D). Note that the spacing is additively associated with far-field voltages (ex. G13(0.31mV)=G12 (0.15mV)+G23 (0.16mV), G15 (0.67mV)=G13 (0.31mV)+G35 (0.36mV)…). P;pacing artifact

Figure 6:The relationship between voltage and spacing in purely healthy area.
Voltage comparison in healthy areas with single component signal between three different spacings (A). the relationship between additive bipolar voltage of Bi-2 and the bipolar voltage of Bi-4 (B) and Bi-8(C). An example of the voltage comparison in one acquisition where all of electrodes 1-5 on one spline (spline-A) were located in a healthy area (D). P;pacing artifact

Supplemental figure.
The catheter placement in each beat is visualized and the proximity indicator (green circle) demonstrates that the active enguide electrode is in contact. Additionally, the system allows users to identify successfully projected points (red dots) under the user-specific definition.

Figure 1.

(A) HD-32 Grid™ catheter

Bi-8 Bi-4 Bi-2

1 segment

1 site

3 mm (edge-edge), 4 mm (center-center)

1 mm (edge-edge)
2 mm (center-center)

Electrode size:

φ 0.80mm, length 1mm

Spline: Each 8 electrodes

HD-32 (4 splines)

HD-56 (7 splines)

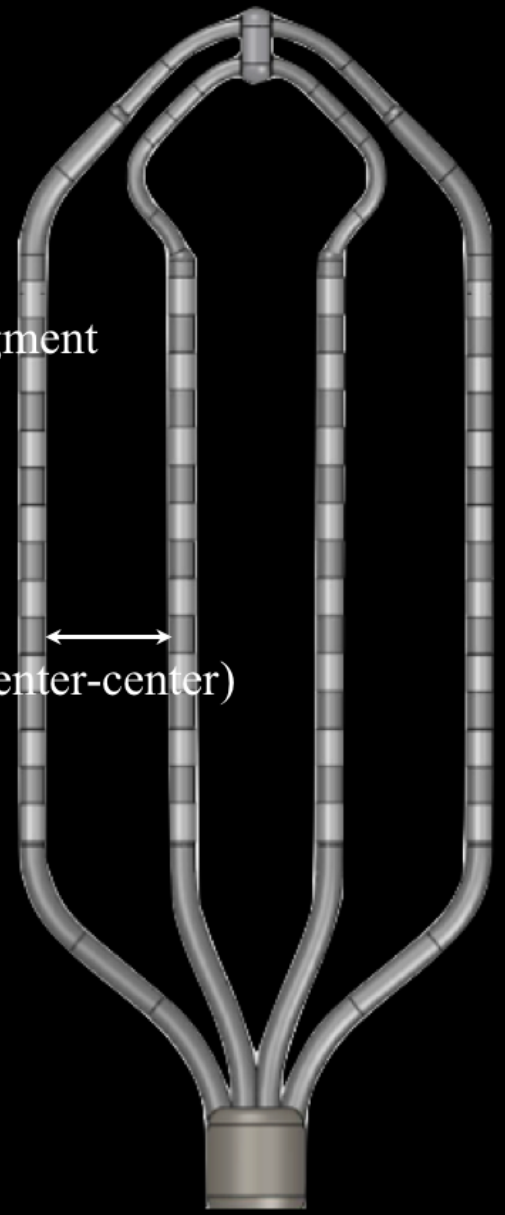

(B)

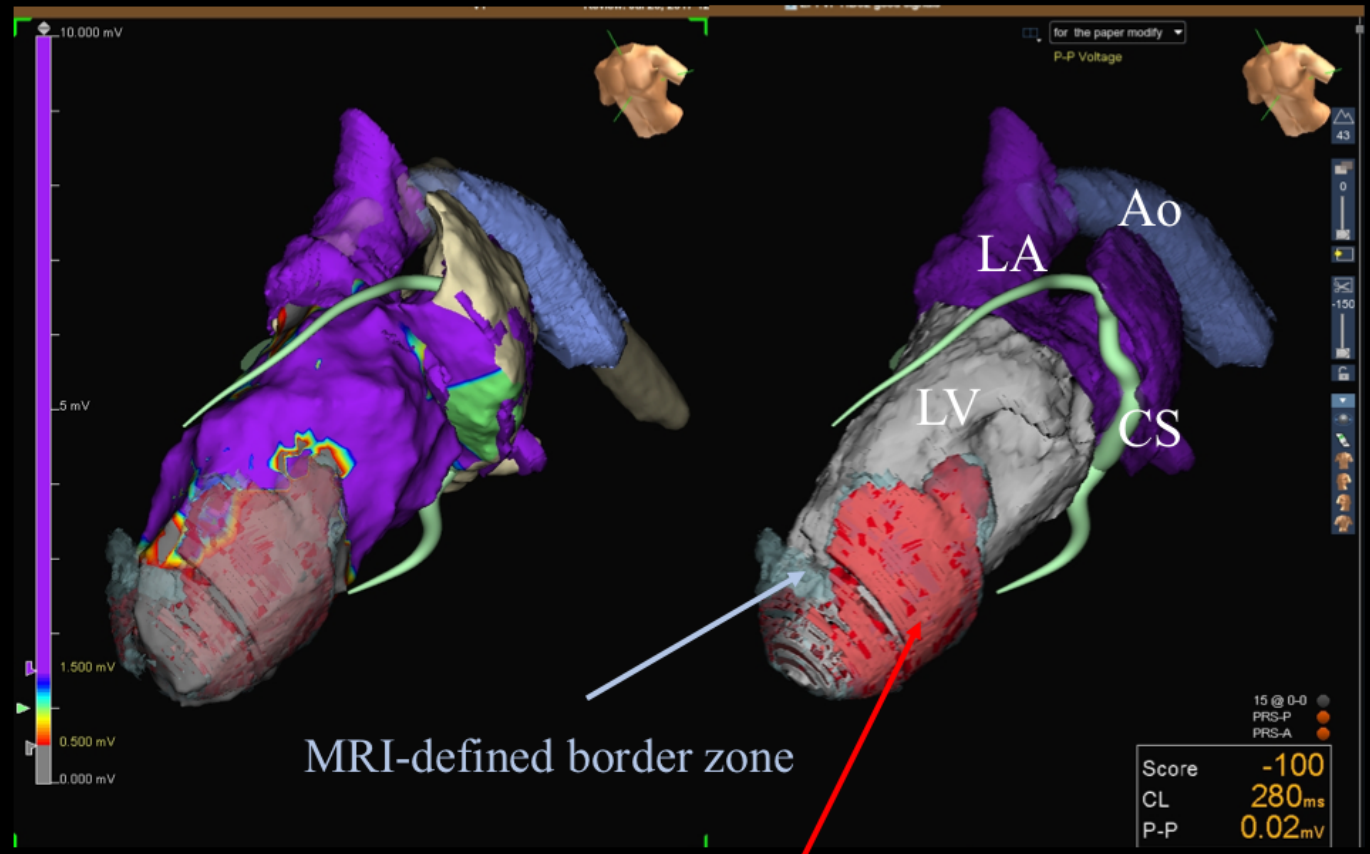

MRI-defined scar area

Figure 2.

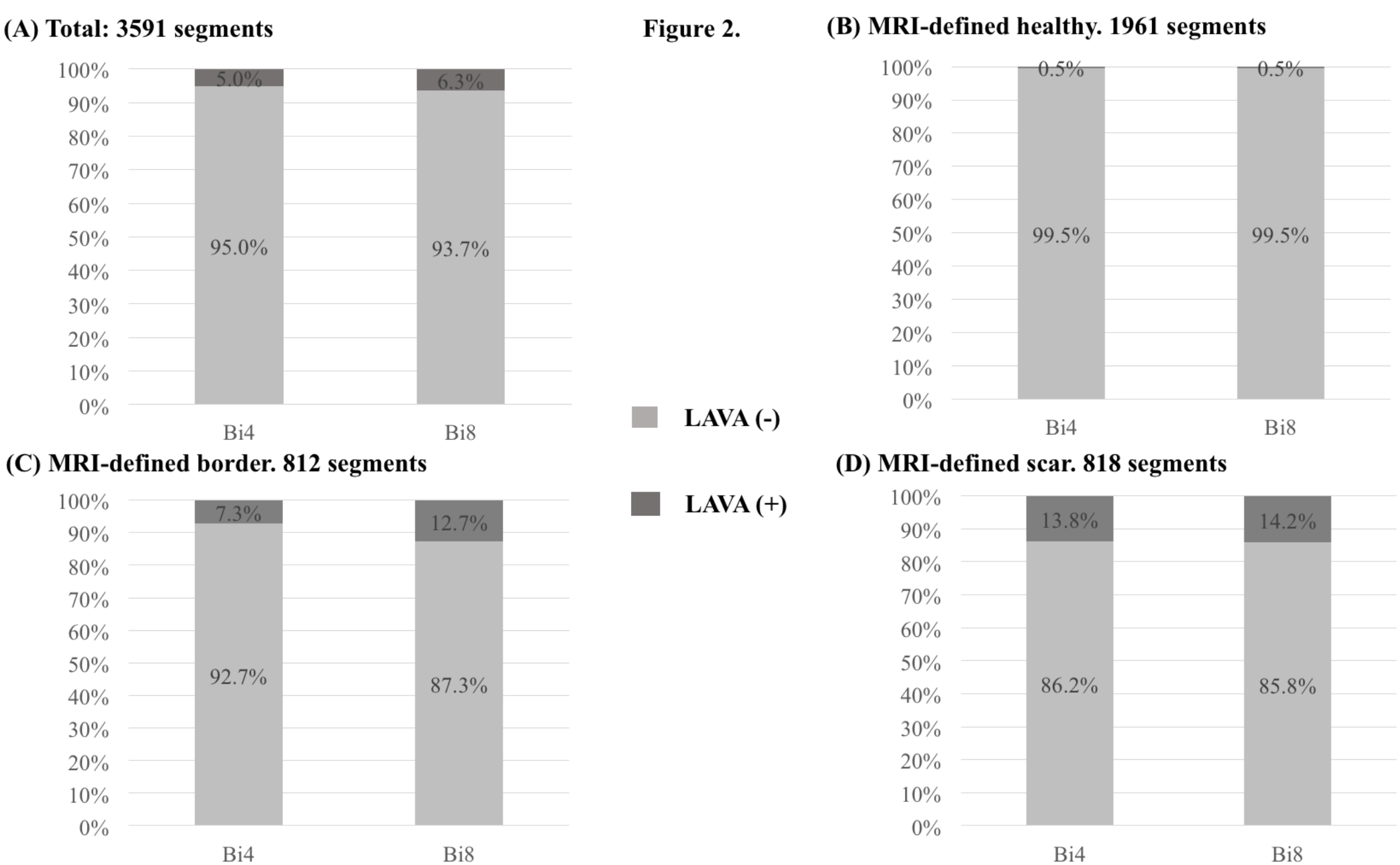
(A) Total: 3591 segments
100%
90%
80%
70%
60%
50%
40%
30%
20%
10%
0%
5.0%
6.3%
95.0%
93.7%
Bi4
Bi8
(B) MRI-defined healthy. 1961 segments
0.5%
0.5%
99.5%
99.5%
Bi4
Bi8
LAVA (-)
LAVA (+)
(C) MRI-defined border. 812 segments
7.3%
12.7%
92.7%
87.3%
Bi4
Bi8
(D) MRI-defined scar. 818 segments
13.8%
14.2%
86.2%
85.8%
Bi4
Bi8

Figure 2E.

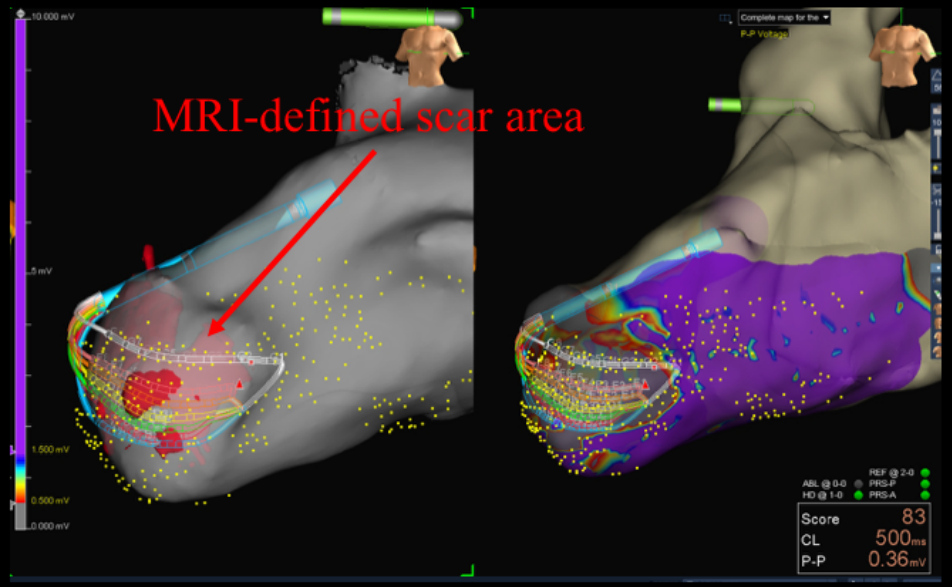

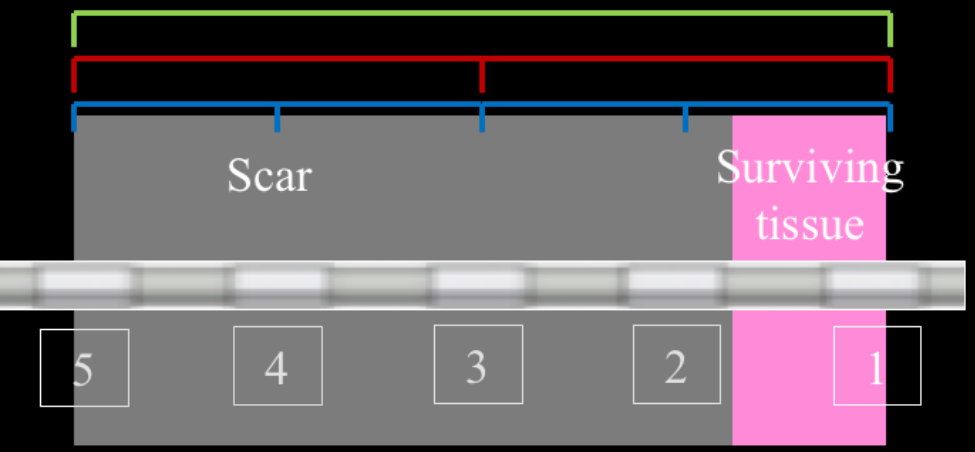

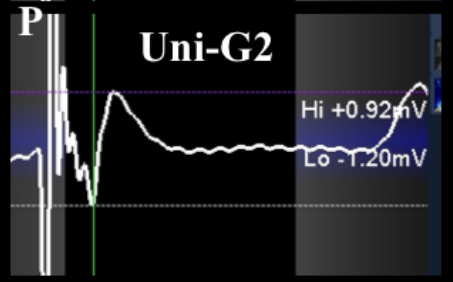

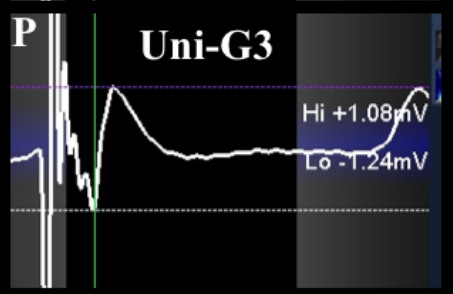

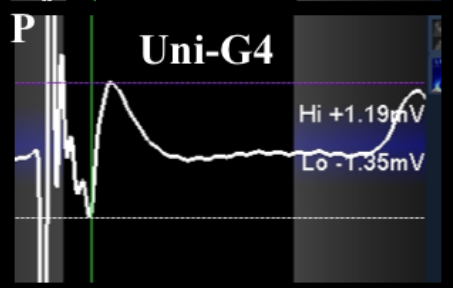

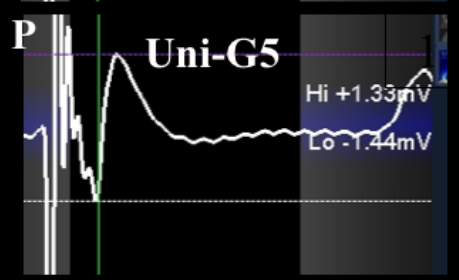

Bipolar configuration

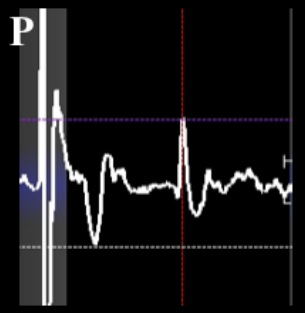

G12
LAVA(+)
Far;0.13mV
Near;0.13mV
Near/Far; 1.0

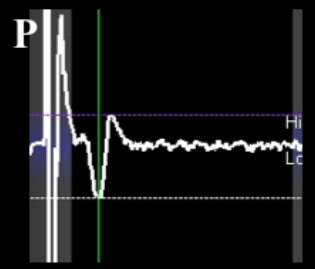

G23 LAVA(-)
Far;0.13mV
Near;0mV

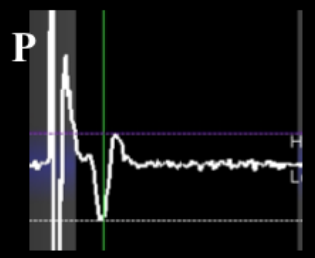

G34 LAVA(-)
Far;0.13mV
Near;0mV

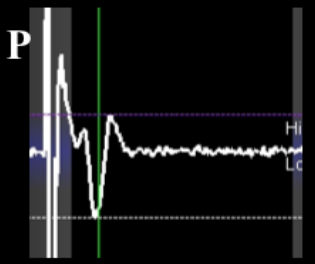

G45 LAVA(-)
Far;0.15mV
Near;0mV

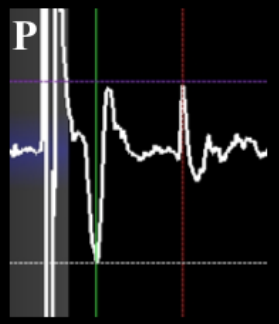

G13 LAVA(+)
Far;0.25mV
Near;0.14mV
Near/Far; 0.56

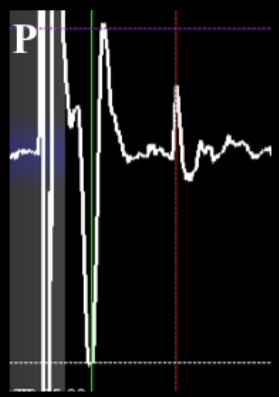

G15 LAVA(+)
Far;0.49mV
Near;0.15mV
Near/Far; 0.31

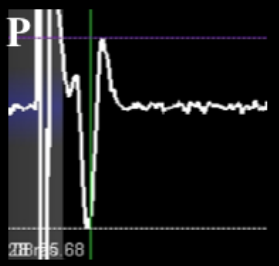

G35 LAVA(-)
Far;0.28mV
Near;0mV

Figure 3.

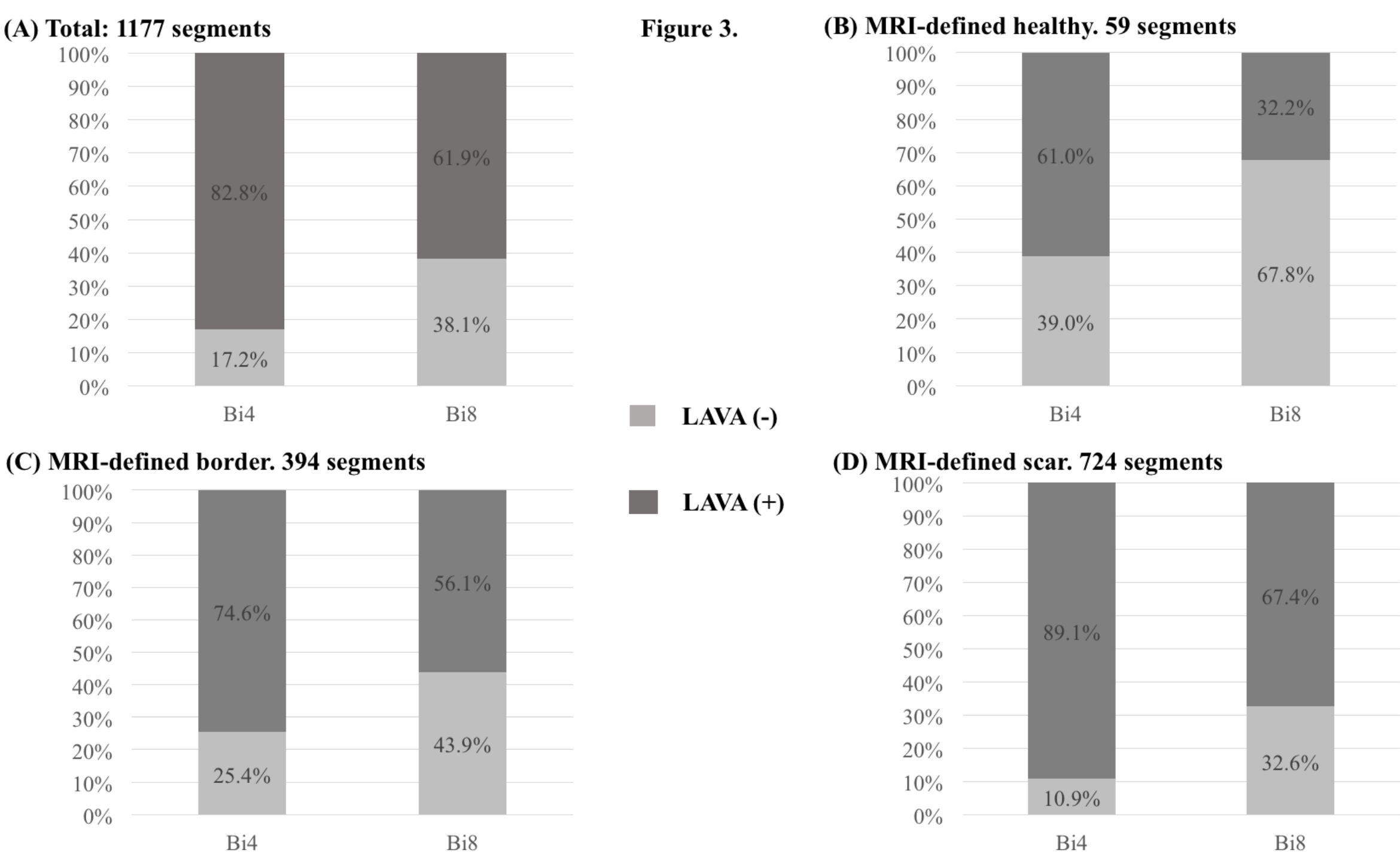
(A) Total: 1177 segments
100%
90%
80%
70%
60%
50%
40%
30%
20%
10%
0%
82.8%
17.2%
61.9%
38.1%
Bi4
Bi8
(B) MRI-defined healthy. 59 segments
61.0%
39.0%
32.2%
67.8%
Bi4
Bi8
LAVA (-)
LAVA (+)
(C) MRI-defined border. 394 segments
74.6%
25.4%
56.1%
43.9%
Bi4
Bi8
(D) MRI-defined scar. 724 segments
89.1%
10.9%
67.4%
32.6%
Bi4
Bi8

Figure 3E.

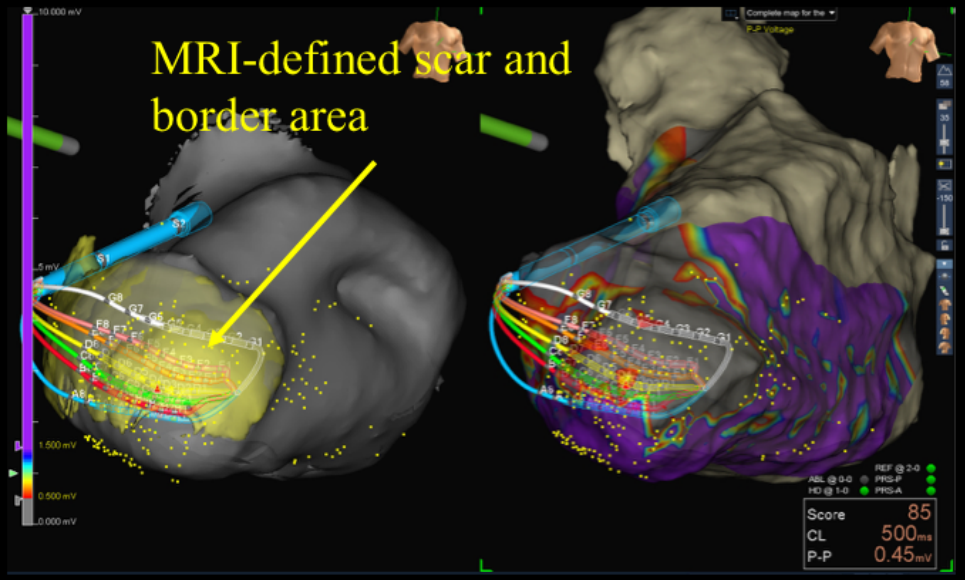

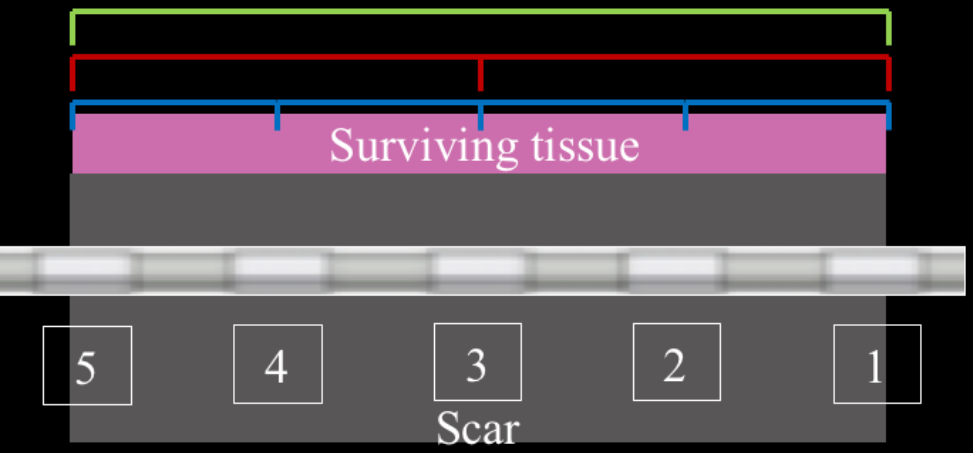

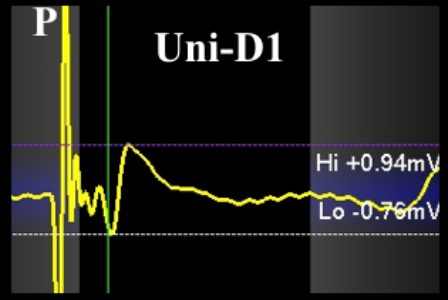

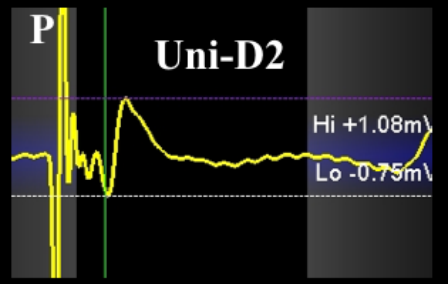

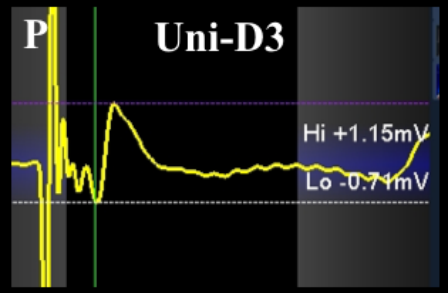

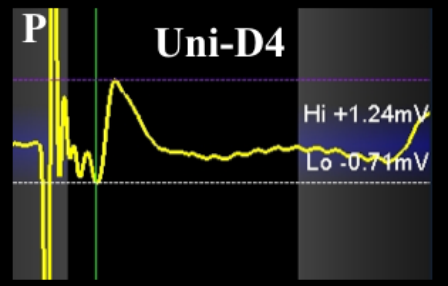

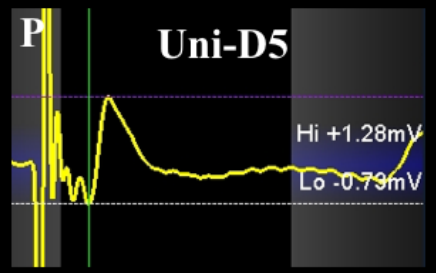

Bipolar configuration

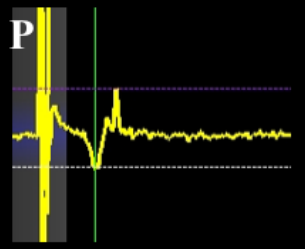

D12 LAVA(+)
Far;0.12mV
Near;0.07mV

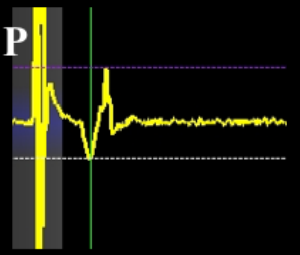

D23 LAVA(+)
Far;0.13mV
Near;0.06mV

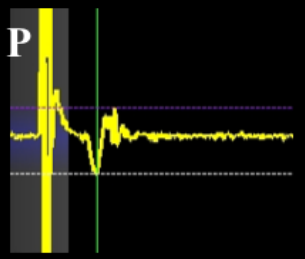

D34 LAVA(+)
Far;0.13mV
Near;0.06mV

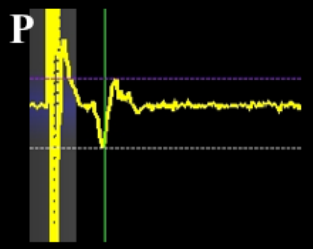

D45 LAVA(+)
Far;0.15mV
Near;0.02mV

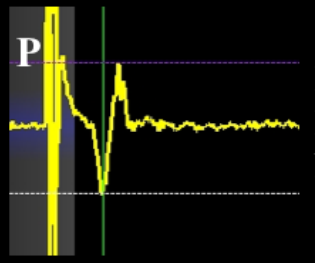

D13 LAVA(+)
Far;0.21mV
Near;0.09mV

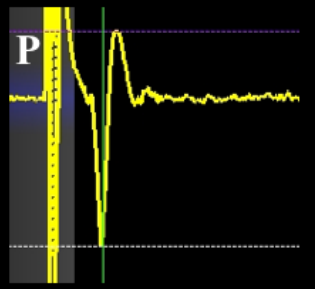

D15 LAVA(-)
Far;0.45mV
Near;0mV

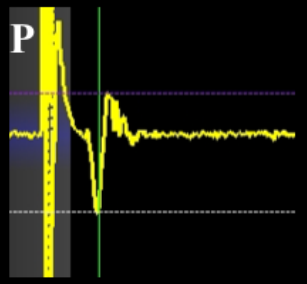

D35
LAVA(+)
Far;0.25mV
Near;0.09mV

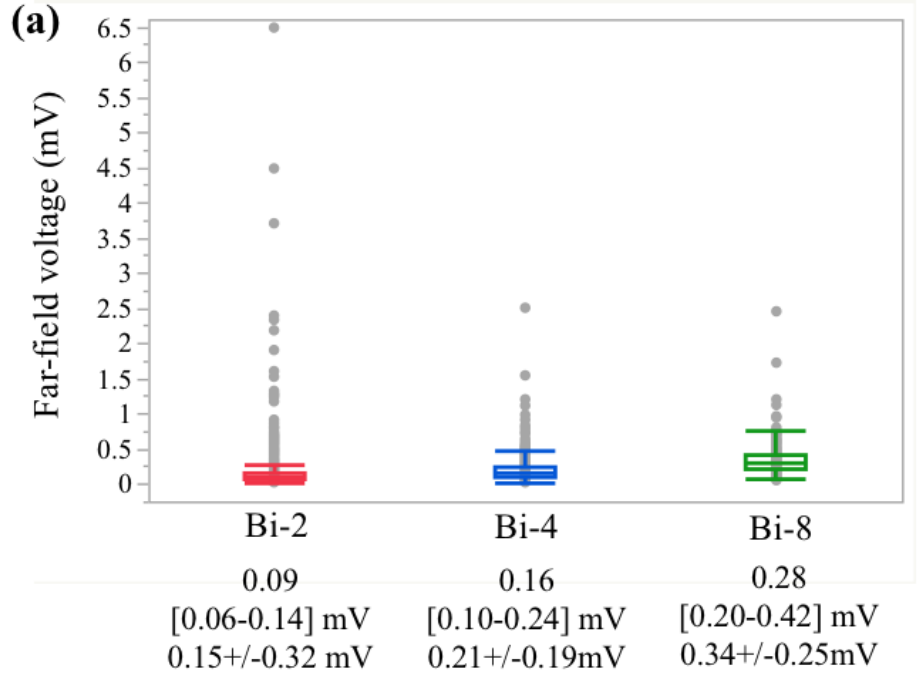

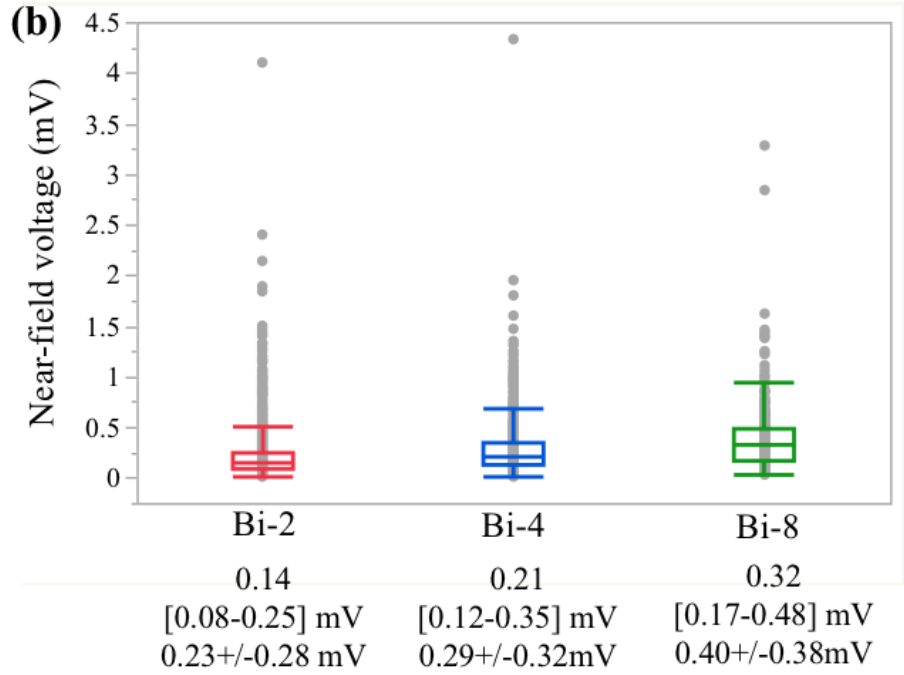

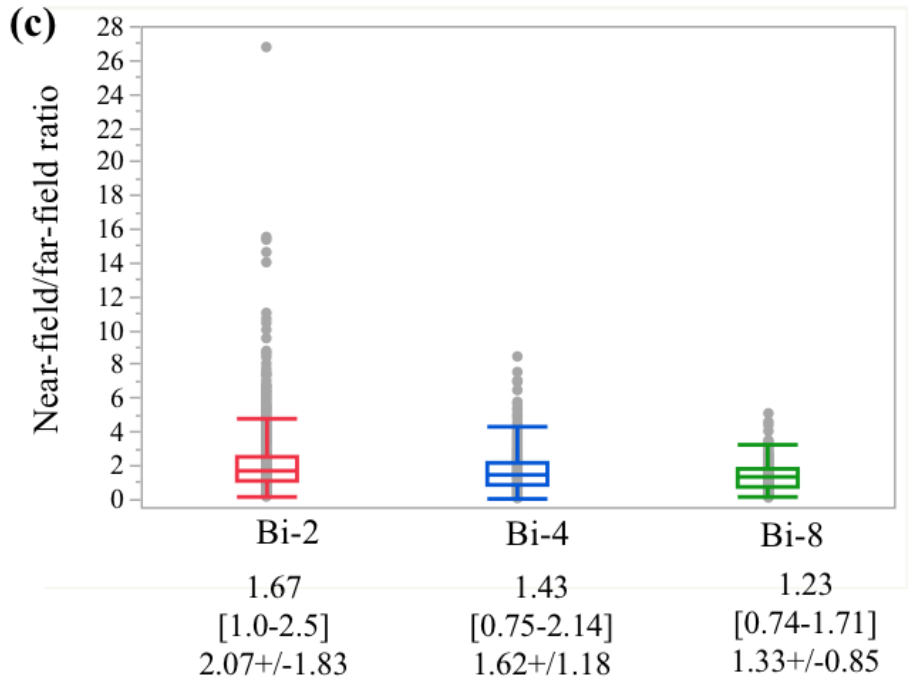

(a) Bi-2 vs Bi-4 (P<0.0001)
Bi-4 vs Bi-8 (P<0.0001)
Bi-2 vs Bi-8 (P<0.0001)

(b) Bi-2 vs Bi-4 (P<0.0001)
Bi-4 vs Bi-8 (P<0.0001)
Bi-2 vs Bi-8 (P<0.0001)

(c) Bi-2 vs Bi-4 (P<0.0001)
Bi-4 vs Bi-8 (P<0.0001)
Bi-2 vs Bi-8 (P<0.0001)

Figure 4A.

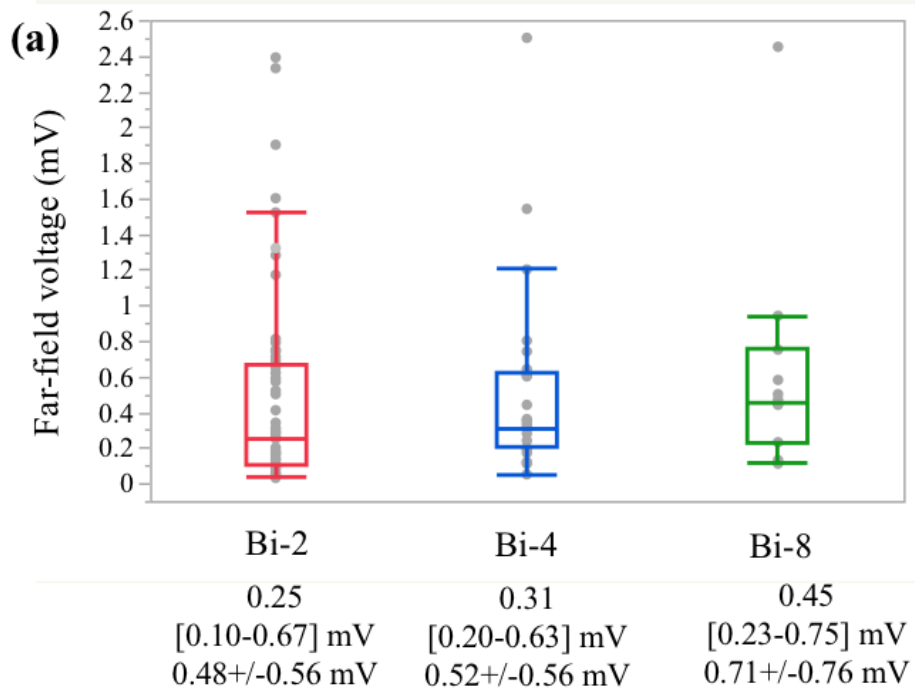

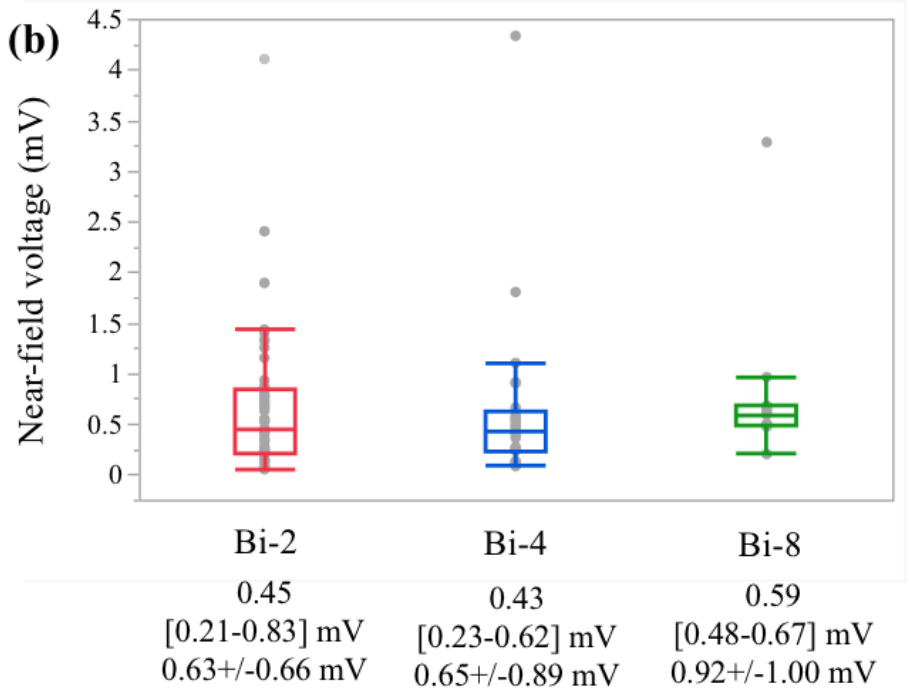

(a) Bi-2 vs Bi-4 (P=0.46)
Bi-4 vs Bi-8 (P=0.38)
Bi-2 vs Bi-8 (P=0.11)

(b) Bi-2 vs Bi-4 (P=0.9)
Bi-4 vs Bi-8 (P=0.04)
Bi-2 vs Bi-8 (P=0.26)

(c) Bi-2 vs Bi-4 (P=0.15)
Bi-4 vs Bi-8 (P=0.97)
Bi-2 vs Bi-8 (P=0.22)

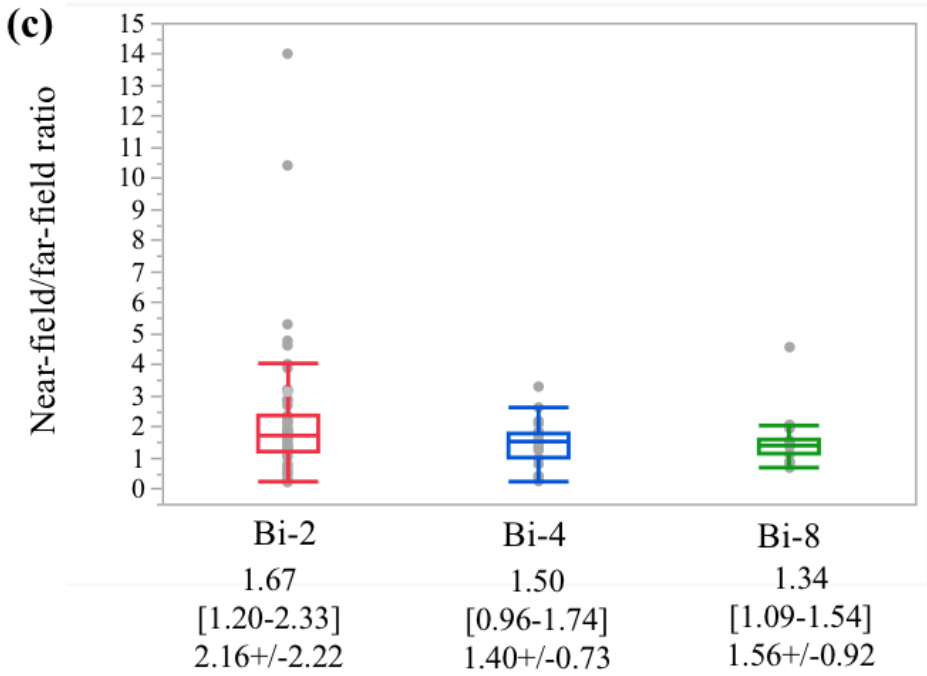

Figure 4B.

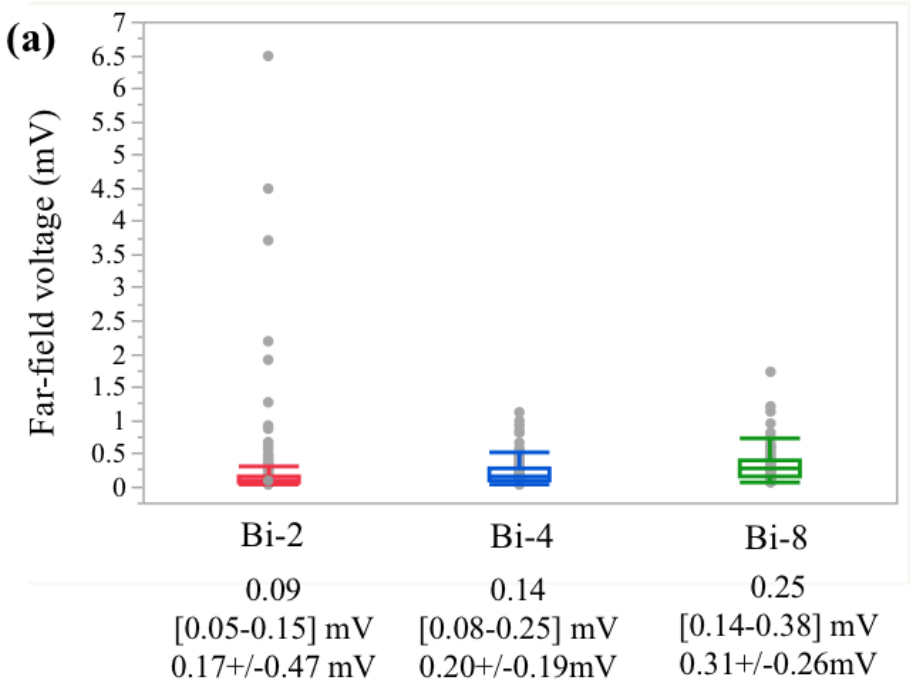

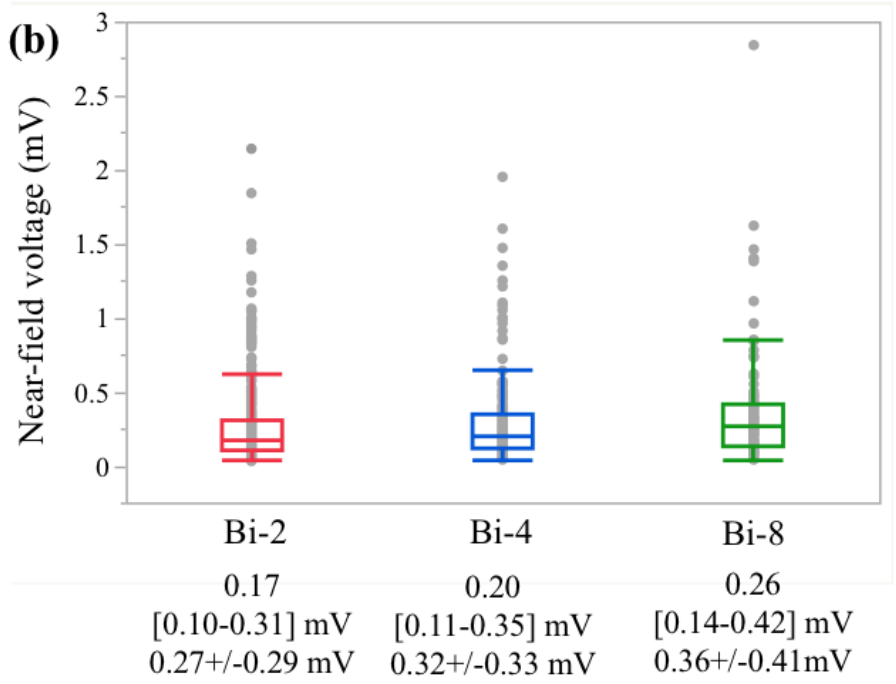

(a) Bi-2 vs Bi-4 (P<0.0001)
Bi-4 vs Bi-8 (P<0.0001)
Bi-2 vs Bi-8 (P<0.0001)

(b) Bi-2 vs Bi-4 (P=0.07)
Bi-4 vs Bi-8 (P=0.05)
Bi-2 vs Bi-8 (P<0.0001)

(c) Bi-2 vs Bi-4 (P<0.0001)
Bi-4 vs Bi-8 (P<0.0001)
Bi-2 vs Bi-8 (P<0.0001)

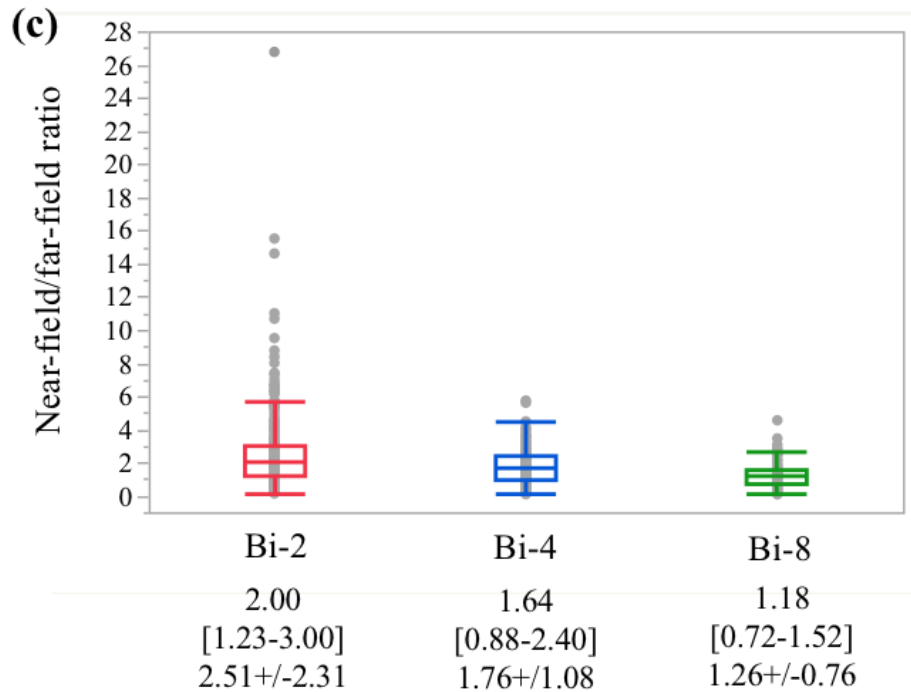

Figure 4C.

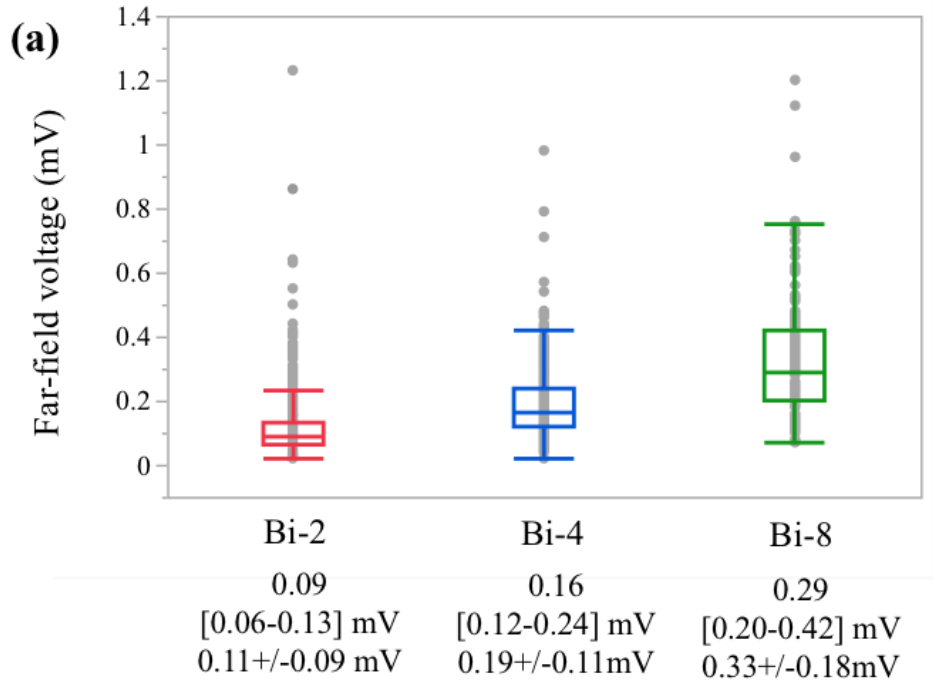

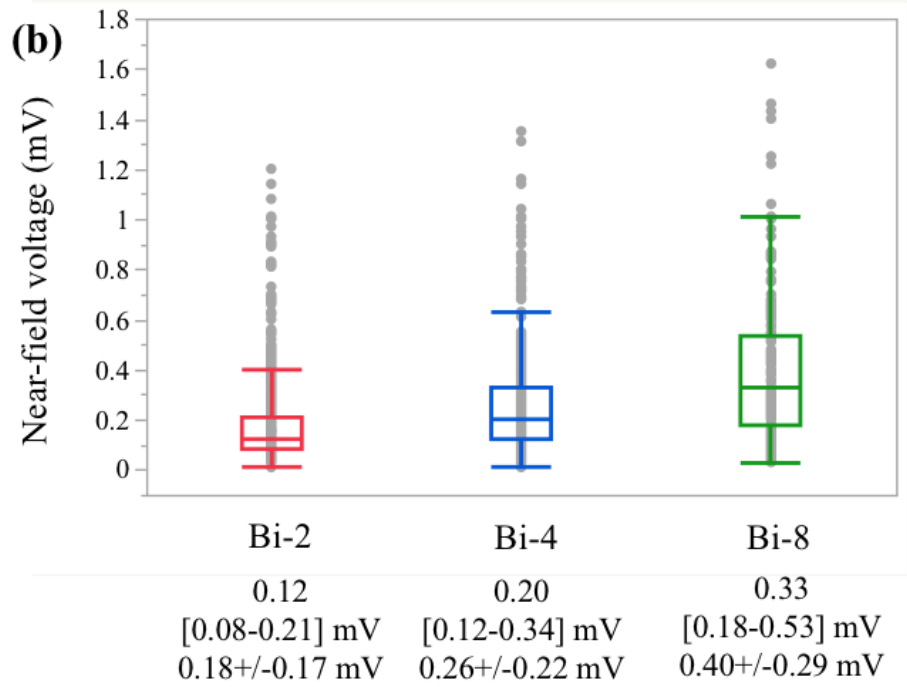

(a) Bi-2 vs Bi-4 (P<0.0001)
Bi-4 vs Bi-8 (P<0.0001)
Bi-2 vs Bi-8 (P<0.0001)

(b) Bi-2 vs Bi-4 (P<0.0001)
Bi-4 vs Bi-8 (P<0.0001)
Bi-2 vs Bi-8 (P<0.0001)

(c) Bi-2 vs Bi-4 (P<0.0001)
Bi-4 vs Bi-8 (P=0.08)
Bi-2 vs Bi-8 (P<0.0001)

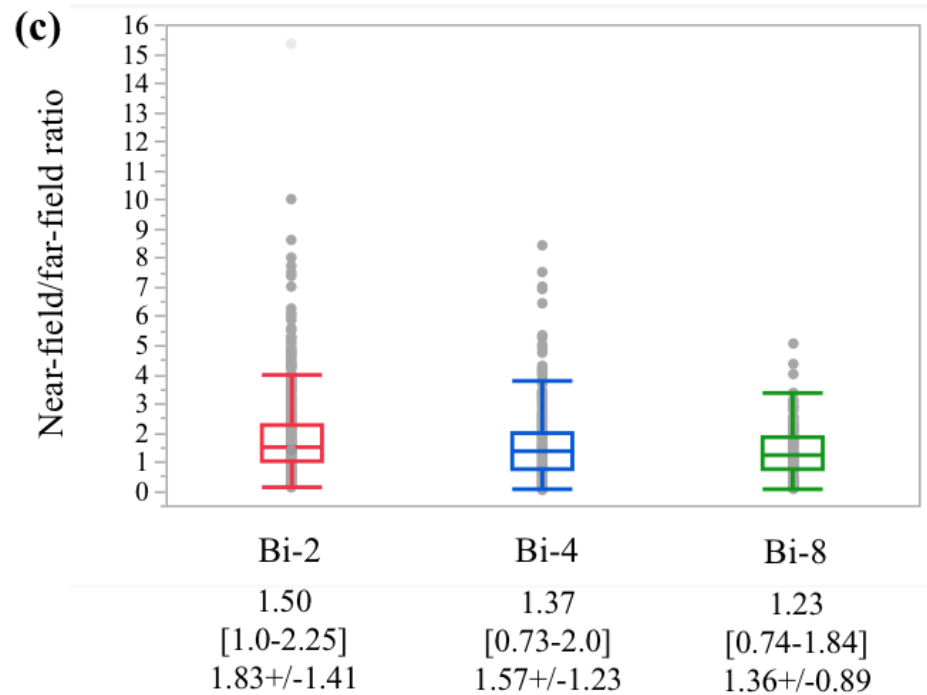

Figure 4D.

Figure 5.

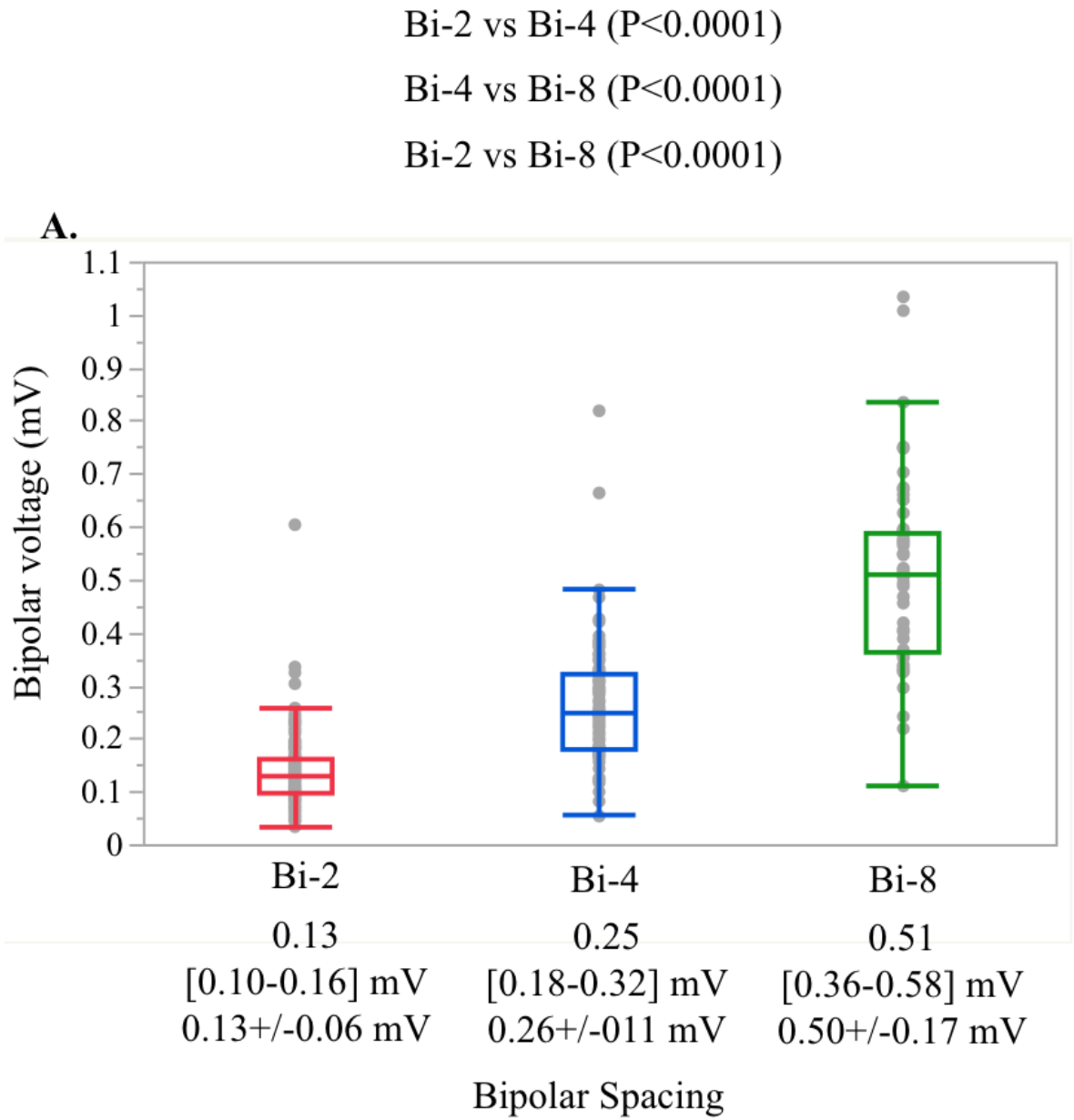
Bi-2 vs Bi-4 (P<0.0001)
Bi-4 vs Bi-8 (P<0.0001)
Bi-2 vs Bi-8 (P<0.0001)
A.
Bipolar voltage (mV)
1.1
1
0.9
0.8
0.7
0.6
0.5
0.4
0.3
0.2
0.1
0
Bi-2
Bi-4
Bi-8
0.13
0.25
0.51
[0.10-0.16] mV
[0.18-0.32] mV
[0.36-0.58] mV
0.13+/-0.06 mV
0.26+/-011 mV
0.50+/-0.17 mV
Bipolar Spacing

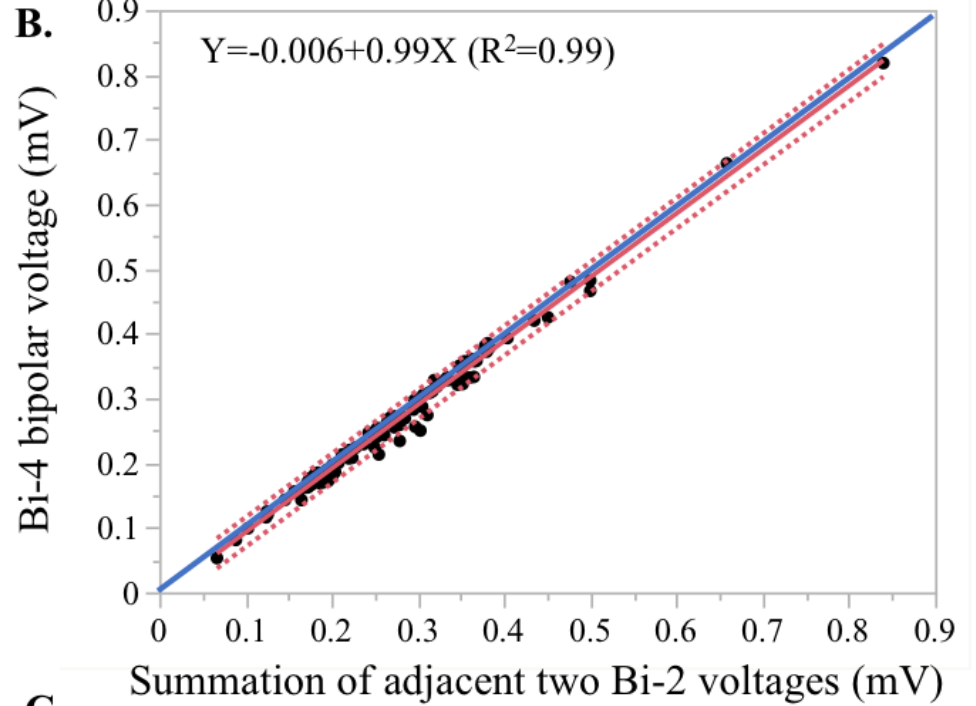
B.
Y=-0.006+0.99X (R²=0.99)
Bi-4 bipolar voltage (mV)
0.9
0.8
0.7
0.6
0.5
0.4
0.3
0.2
0.1
0
0 0.1 0.2 0.3 0.4 0.5 0.6 0.7 0.8 0.9
Summation of adjacent two Bi-2 voltages (mV)

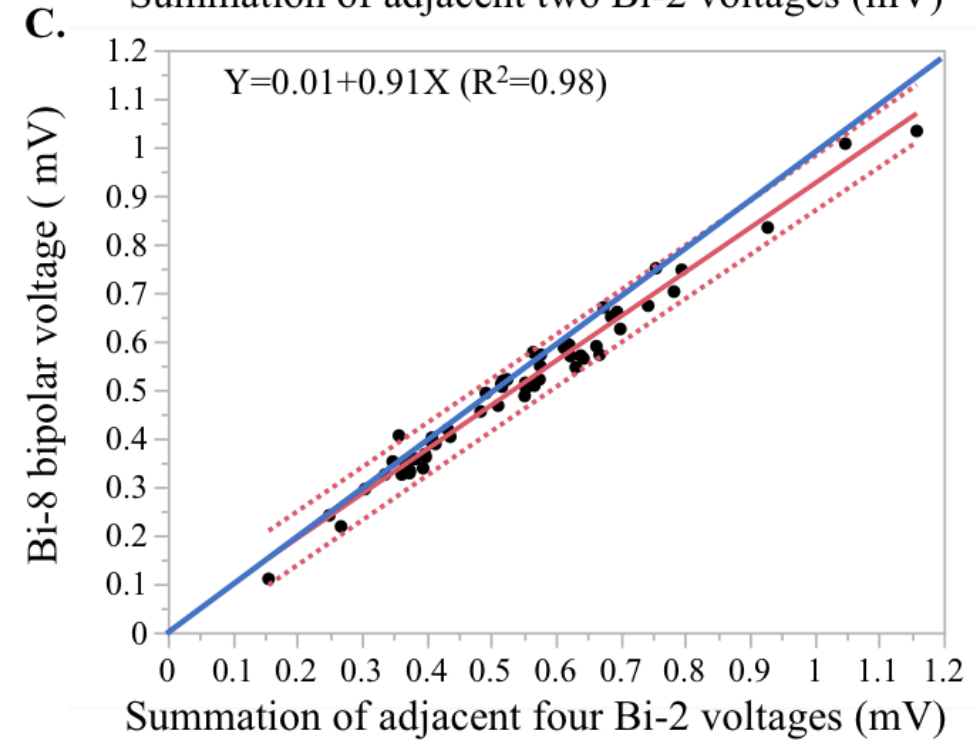
C.
Y=0.01+0.91X (R²=0.98)
Bi-8 bipolar voltage (mV)
1.2
1.1
1
0.9
0.8
0.7
0.6
0.5
0.4
0.3
0.2
0.1
0
0 0.1 0.2 0.3 0.4 0.5 0.6 0.7 0.8 0.9 1 1.1 1.2
Summation of adjacent four Bi-2 voltages (mV)

Figure 5D.

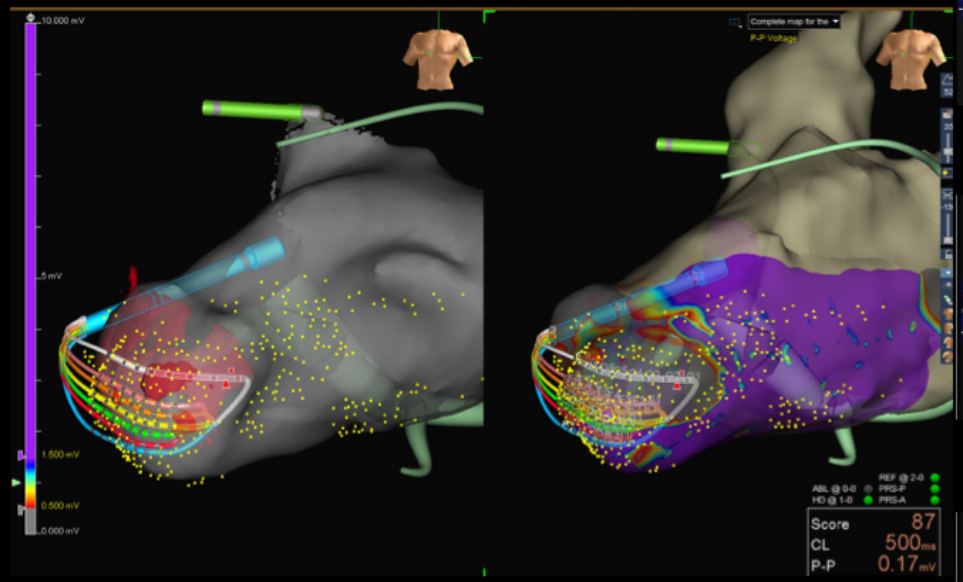

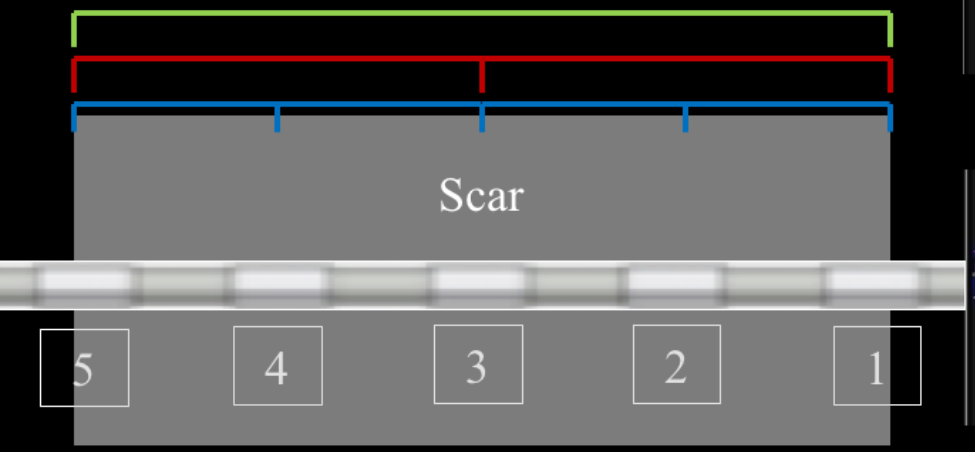

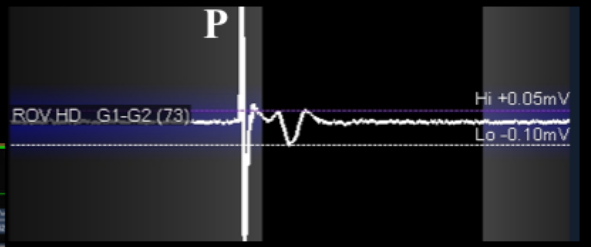

G12 LAVA(-)
Far;0.15mV
Near;0mV

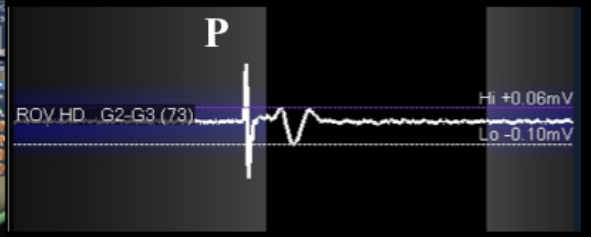

G23 LAVA(-)
Far;0.16mV
Near;0mV

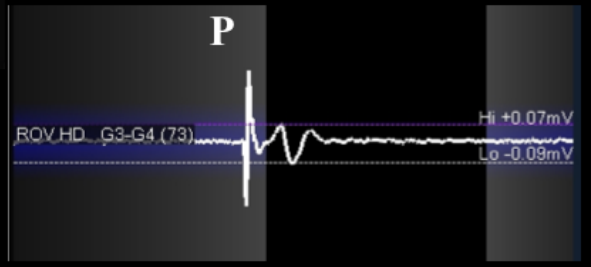

G34 LAVA(-)
Far;0.16mV
Near;0mV

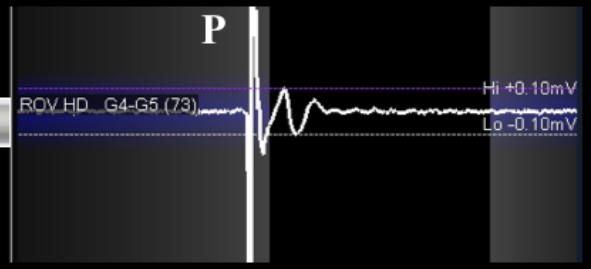

G45 LAVA(-)
Far;0.20mV
Near;0mV

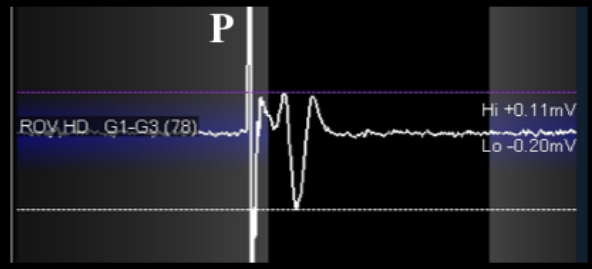

G13 LAVA(+)
Far;0.31mV
Near;0mV

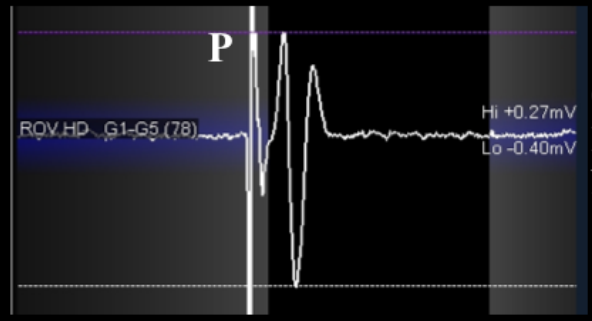

G15 LAVA(-)
Far;0.67mV
Near;0mV

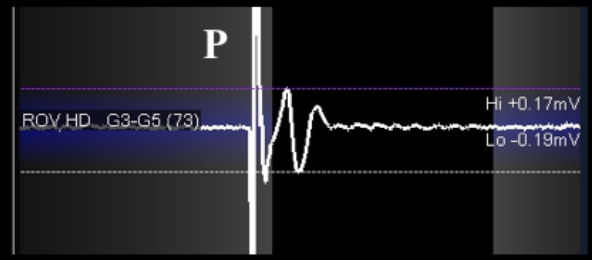

G35
LAVA(+)
Far;0.36mV
Near;0mV

Figure 6.

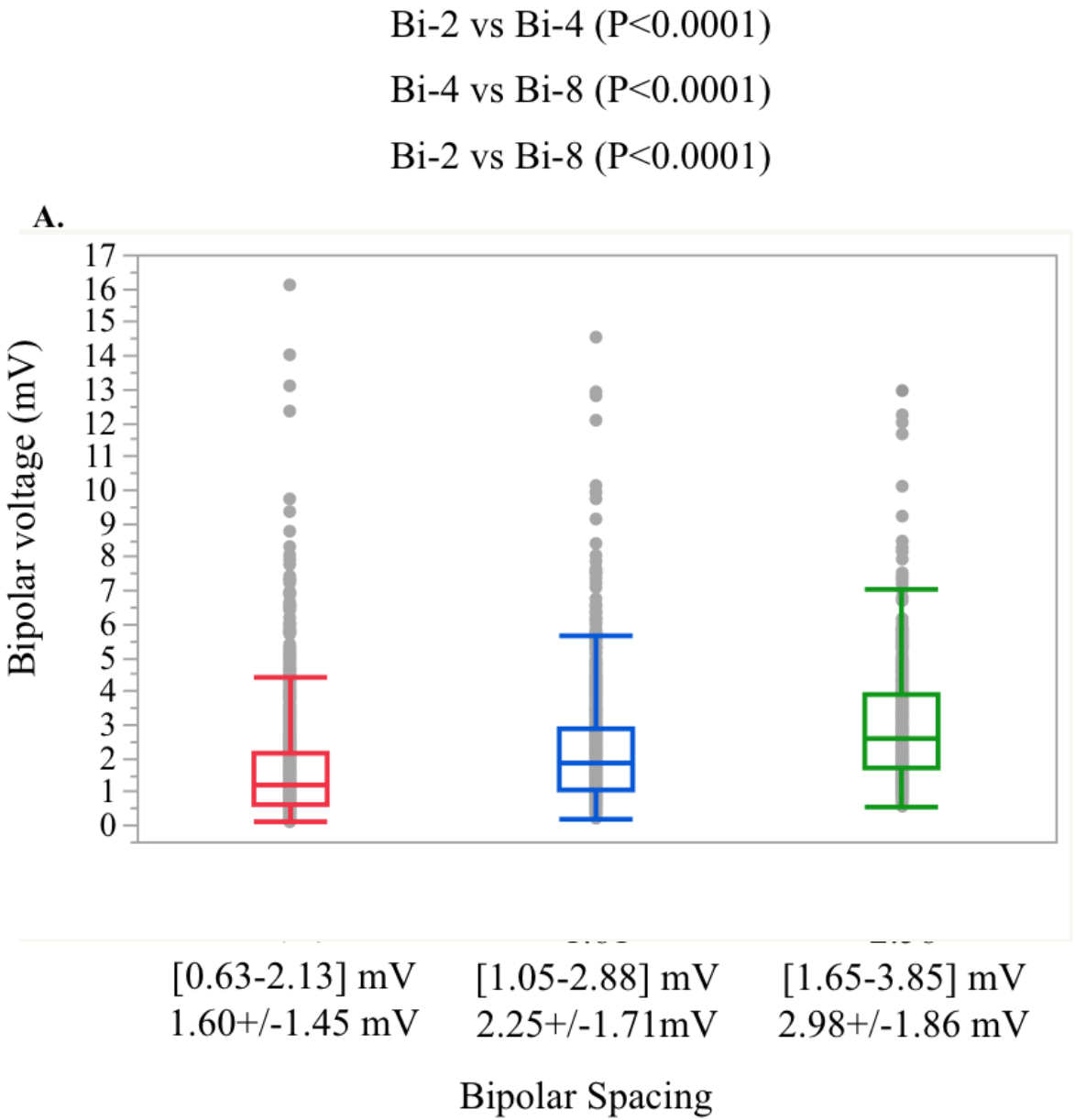
Bi-2 vs Bi-4 (P<0.0001)
Bi-4 vs Bi-8 (P<0.0001)
Bi-2 vs Bi-8 (P<0.0001)
A.
Bipolar voltage (mV)
0
1
2
3
4
5
6
7
8
9
10
11
12
13
14
15
16
17
[0.63-2.13] mV
1.60+/-1.45 mV
[1.05-2.88] mV
2.25+/-1.71mV
[1.65-3.85] mV
2.98+/-1.86 mV
Bipolar Spacing

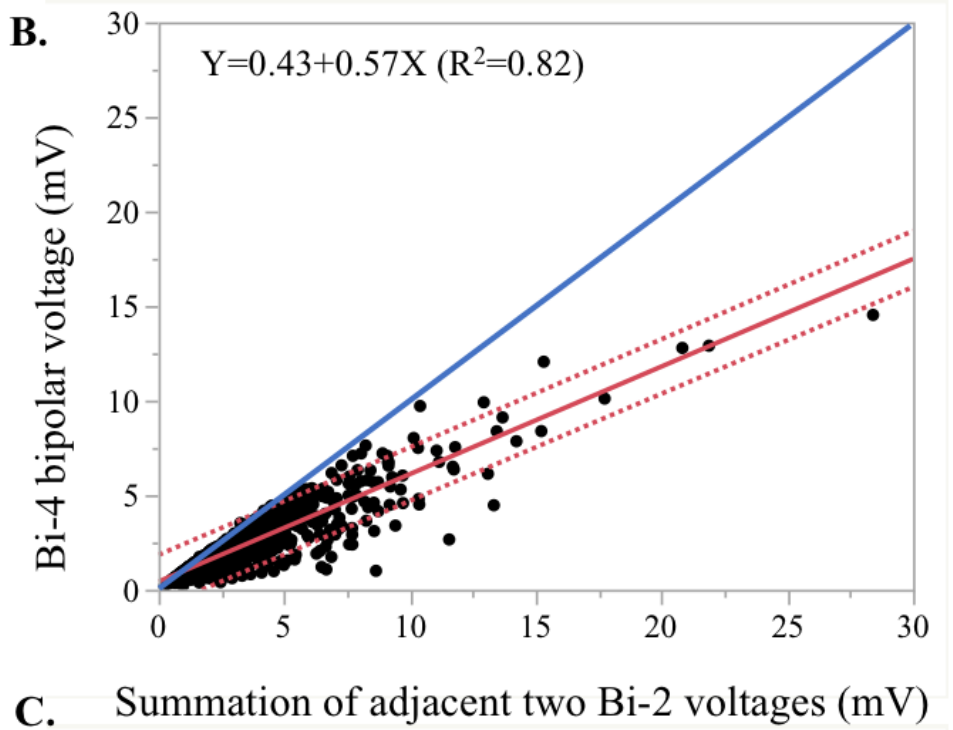
B.
Y=0.43+0.57X (R²=0.82)
Bi-4 bipolar voltage (mV)
0
5
10
15
20
25
30
Summation of adjacent two Bi-2 voltages (mV)

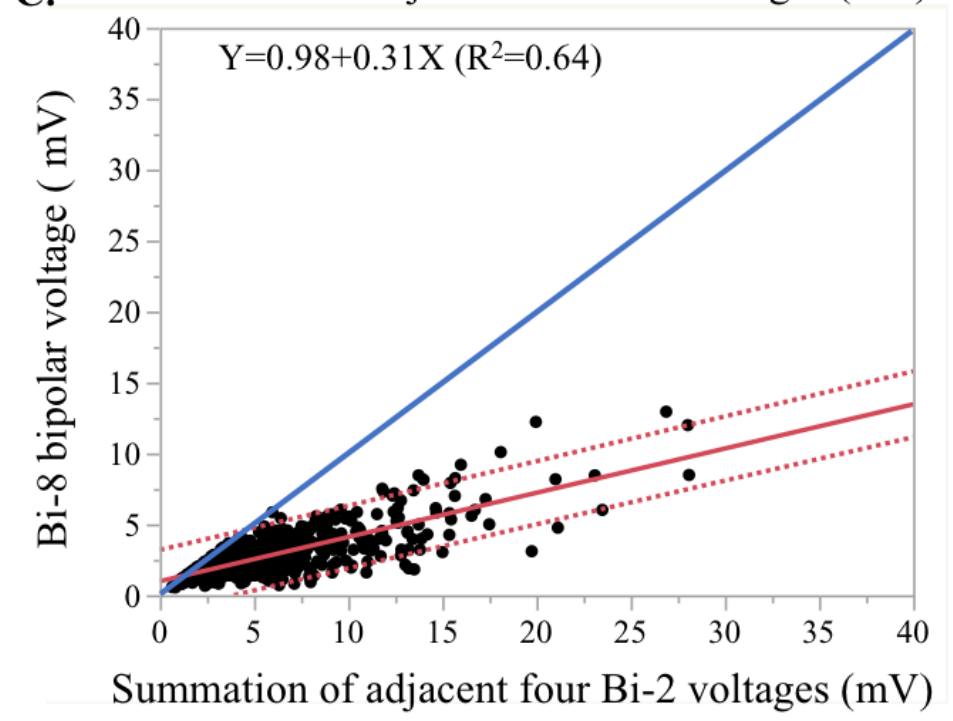
C.
Y=0.98+0.31X (R²=0.64)
Bi-8 bipolar voltage (mV)
0
5
10
15
20
25
30
35
40
Summation of adjacent four Bi-2 voltages (mV)

Figure 6D.

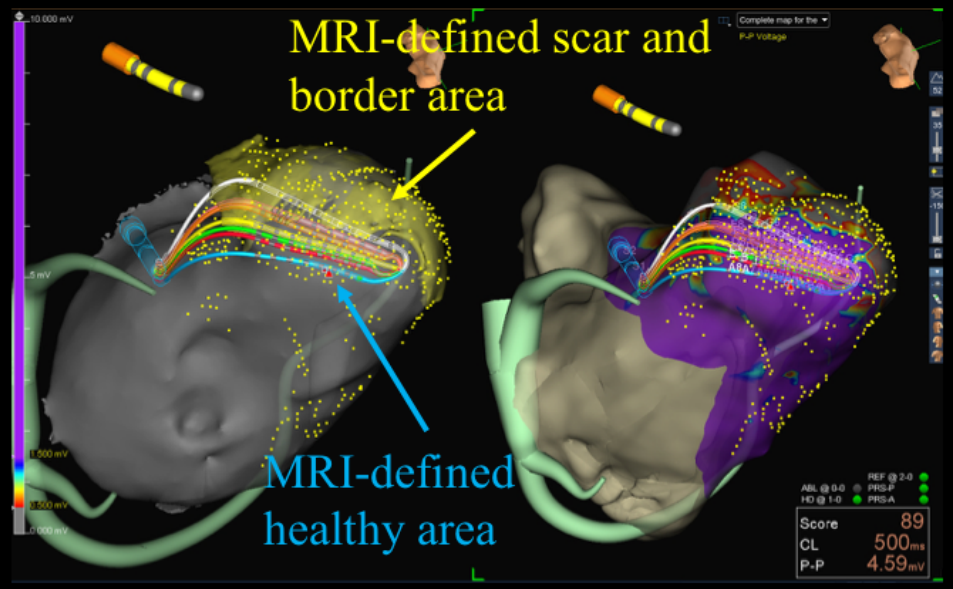

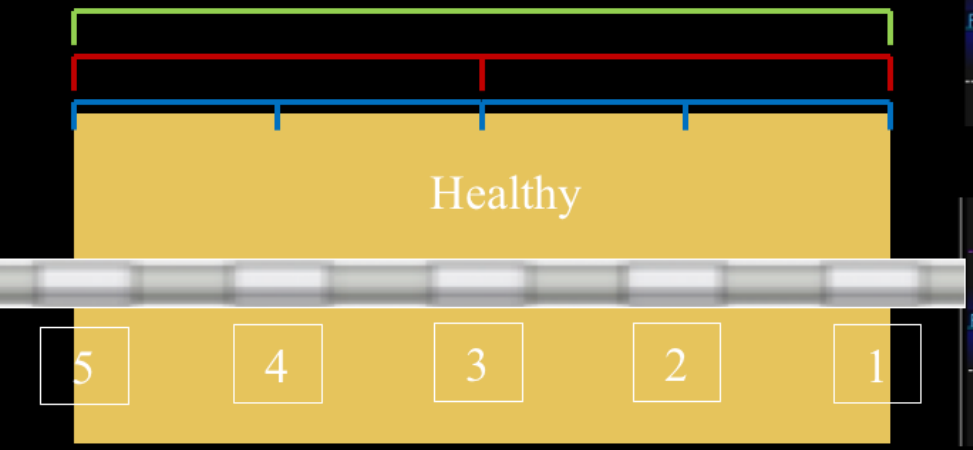

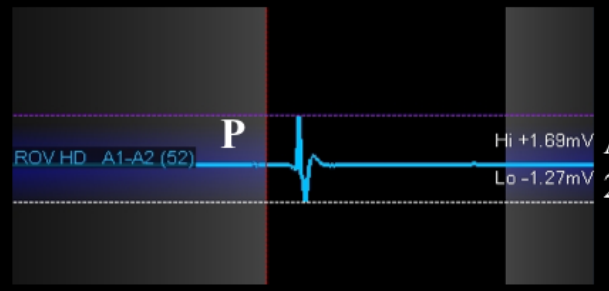

A12 LAVA(-)
2.96mV

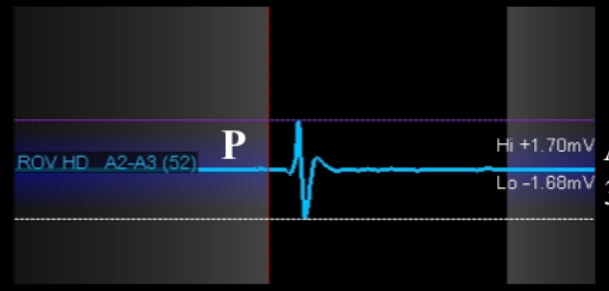

A23 LAVA(-)
3.38mV

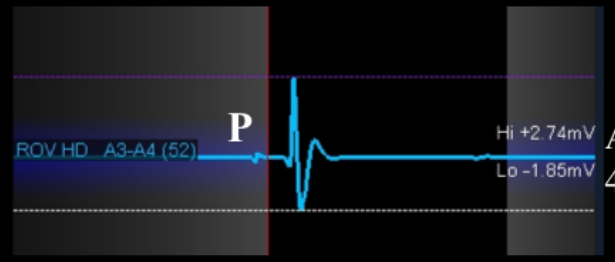

A34 LAVA(-)
4.59mV

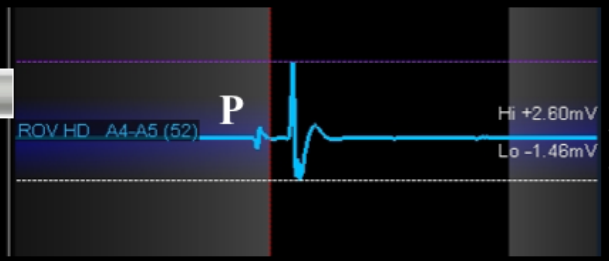

A45 LAVA(-)
4.06mV

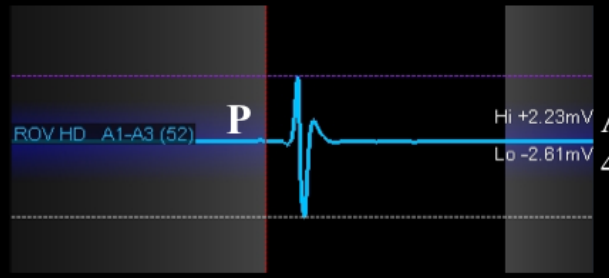

A13 LAVA(-)
4.84mV

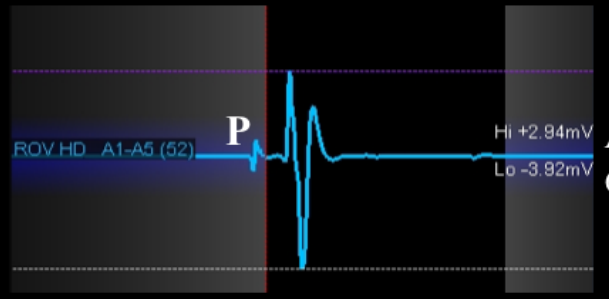

A15 LAVA(-)
6.86mV

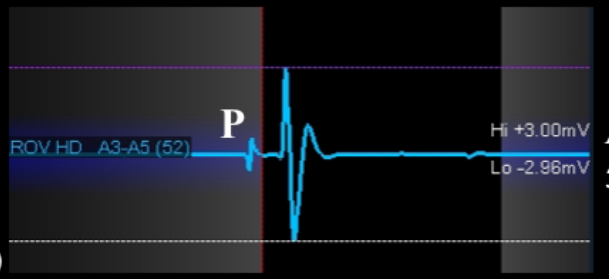

A35 LAVA(-)
5.96mV

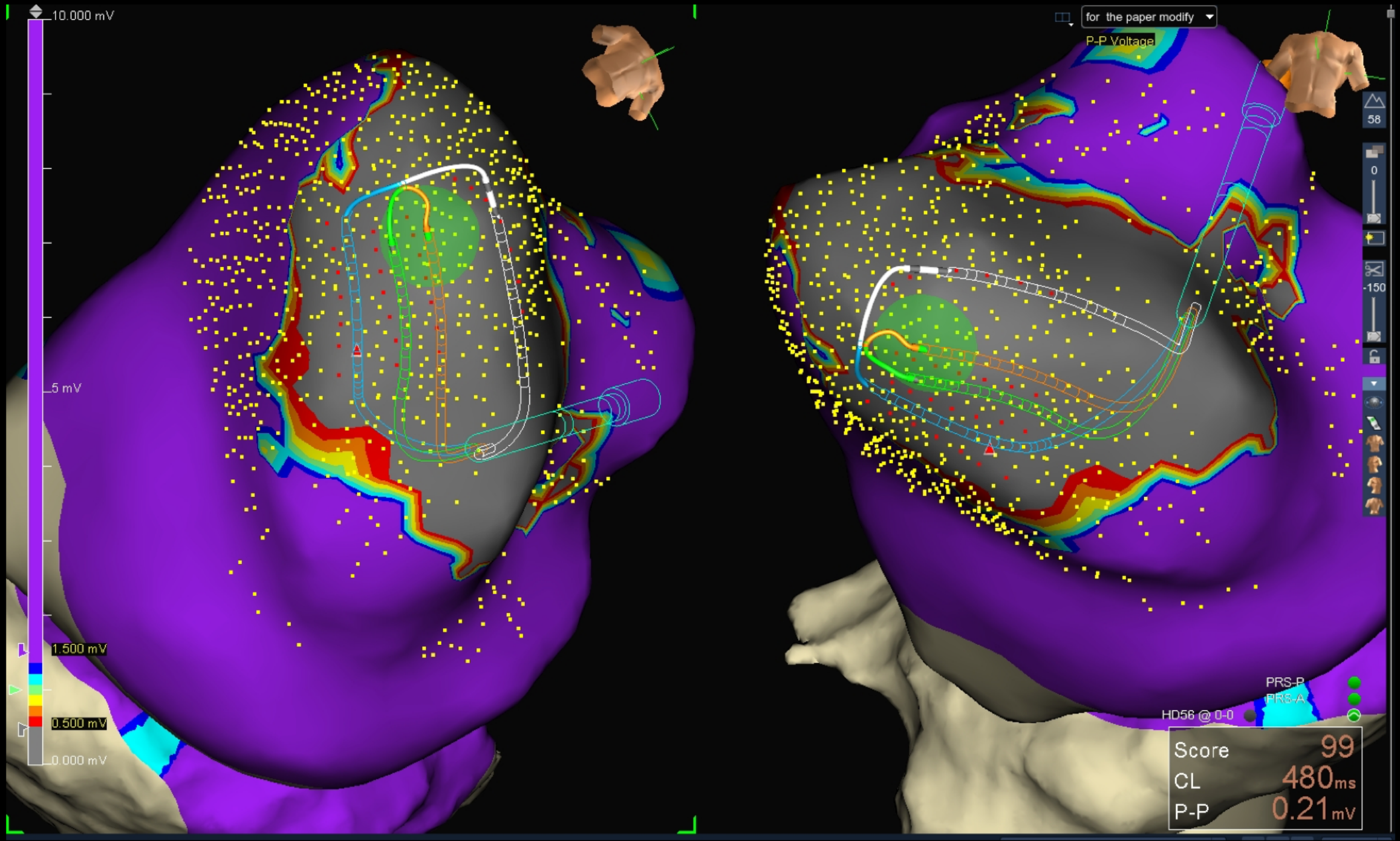
10.000 mV
5 mV
1.500 mV
0.500 mV
0.000 mV
for the paper modify
P-P Voltage
58
0
-150
PRS-P
PRS-A
HD56 @ 0-0
Score 99
CL 480ms
P-P 0.21mV